REPORT 1249

A UNIFIED TWO-DIMENSIONAL APPROACH TO THE CALCULATION OF THREE-DIMENSIONAL HYPERSONIC FLOWS, WITH APPLICATION TO BODIES OF REVOLUTION [1]

By A. J. Eggers, Jr., and Raymond C. Savin

SUMMARY

A simplified two-dimensional method for calculating three-dimensional steady and nonsteady hypersonic flows of an inviscid (non-heat-conducting) gas is deduced from characteristics theory. This method is appropriately termed a generalized shock-expansion method. It is demonstrated that the method is applicable when disturbances associated with the divergence of streamlines in planes tangent to a surface are of secondary importance compared to those associated with the curvature of streamlines in planes normal to the surface. When this condition is met, surface streamlines may be treated as geodesics, which, in turn, may be related to the geometry of the surface.

It is inquired further if the two-dimensionality of inviscid hypersonic flows has a counterpart in hypersonic boundary-layer flows. This question is answered in the affirmative, thereby permitting a unified two-dimensional approach to three-dimensional hypersonic flows.

This concept is applied to bodies of revolution in steady flight and, with the assumption that flow at the vertex is conical, approximate solutions for the flow field are obtained for values of the hypersonic similarity parameter (i. e., the ratio of the free-stream Mach number to the fineness ratio of the body) greater than about 1 and for small angles of attack. Surface streamlines are approximated by meridian lines and the flow field is calculated in meridian planes. Simple explicit expressions are obtained for the surface Mach numbers and pressures in the special case of slender bodies.

The validity of theory is checked by comparison with surface pressures and shock-wave shapes obtained experimentally at Mach numbers from 3.00 to 6.30 and angles of attack up to 15° for two ogives having fineness ratios of 3 and 5. At the lower angles of attack, theory and experiment approach agreement when the hypersonic similarity parameter is in the neighborhood of 1 or greater. At the larger angles of attack, theory tends to break down noticeably on the leeward sides of the bodies.

INTRODUCTION

The calculation of flows about objects, primarily missiles, traveling at high supersonic speeds is now generally accepted as a matter of more than academic interest. The difficulty of these calculations stems in large part from the fact that at such high speeds disturbance velocities are not necessarily small compared to the velocity of sound, nor are entropy gradients necessarily negligible in the disturbed flow field about a body, even though it may be of normal slenderness. Thus, for example, the relatively simple linear theory, which has proven so valuable in studying flows at low supersonic speeds, loses much of its utility in the study of high-supersonic-speed flows. In the quest for methods especially suited to calculating high-supersonic-speed flows, notable progress has been made in the development of similarity laws relating the flows about slender three-dimensional shapes in both steady (see refs. 1, 2, and 3) and nonsteady motion (see refs. 4 and 5). Steady two-dimensional flows have received perhaps the greatest attention from the standpoint of calculating specific flow fields, and it would seem that with tools ranging from the characteristics method (see, e. g., refs. 6 and 7) to the generalized shock-expansion method (ref. 7) the problem is reasonably well in hand, at least insofar as inviscid, continuum flow is concerned. A more or less analogous situation exists with regard to the nonlifting body of revolution (see, e. g., refs. 6, 8, 9, and 10) although it seems that only in the case of the cone has a method (ref. 10) of simplicity comparable to that of the linear theory been developed for calculating the whole flow field.

When one departs from these relatively simple flows, the number of tools for carrying out practical calculations decreases sharply. Thus, for example, in the category of inclined bodies of revolution, it appears that only bodies at small angles of attack have been handled adequately, usually by either the method of characteristics or some other step-by-step calculative procedure (see, e. g., refs. 6, and 11 through 14). In the case of steady flow about general three-dimensional shapes, aside from Newtonian flow concepts, which are strictly applicable at Mach numbers exceeding all limits, only the characteristics method has apparently thus far received serious attention (refs. 15, 16, 17, and 18). It is true, of course, that the method is tedious and time consuming to apply, but the relatively exact solutions obtained provide a valuable check against the predictions of more approximate but simpler theories. In addition, however, as demonstrated in reference 10, a study of the compatibility equations of the characteristics method can prove useful in determining simplified methods for calculating more complex flow fields.

With these points in mind, it is first undertaken in the present report to redevelop characteristics theory in a form which enables us to obtain a simplified two-dimensional method for calculating both steady and nonsteady hypersonic flows about three-dimensional shapes. Viscous flows are then considered and it is demonstrated that the two-dimensional character of inviscid hypersonic flows has a counterpart in hypersonic boundary-layer flows. The validity of the analytical methods of this paper is checked by comparing

[1] Supersedes NACA TN 2811 entitled "On the Calculation of Flow About Objects Traveling at High Supersonic Speeds," by A. J. Eggers, Jr., 1952.

413672—57——75

the predictions of theory with experimental results for the surface pressures and bow shock waves of lifting and nonlifting bodies of revolution at Mach numbers from 3.00 to 6.30.

NOTATION

a	local speed of sound
C_A	axial-force coefficient, $\frac{\text{axial force}}{q_\infty \pi \left(\frac{d^2}{4}\right)}$
C_N	normal-force coefficient, $\frac{\text{normal force}}{q_\infty \pi \left(\frac{d^2}{4}\right)}$
C_m	pitching-moment coefficient, $\frac{\text{moment about body vertex}}{q_\infty \pi \left(\frac{d^2}{4}\right) l}$
c_p	specific heat at constant pressure
c_v	specific heat at constant volume
C_{1z}, C_{2z}	characteristic coordinates in X-Z plane (C_{1z} is positively inclined with respect to X)
C_p	pressure coefficient, $\frac{p-p_\infty}{q_\infty}$
d	maximum diameter of body of revolution
K	hypersonic similarity parameter, $M_\infty \frac{d}{l}$
l	characteristic body length (measured from vertex to most forward point of maximum diameter)
M	Mach number (ratio of local velocity to local speed of sound)
p	static pressure
p_t	total pressure
q_∞	free-stream dynamic pressure
S	entropy
t	time
u, v, w	components of fluid velocity along the X, Y, and Z axes, respectively
x, y, z	rectangular coordinates along the X, Y, and Z axes, respectively
x, r, φ	cylindrical coordinates
$\bar{x}$	center-of-pressure position (measured from body vertex)
α	angle of attack
γ	ratio of specific heats, $\frac{c_p}{c_v}$
δ	angle between X axis and tangent to projection of streamline (or pathline) in X-Z plane
δ_N	semivertex angle of body
Δ	angle between X axis and tangent to projection of streamline (or pathline) in X-Y plane
μ	Mach angle, $\sin^{-1}\frac{1}{M}$
ν	ray angle for Prandtl-Meyer flow
ρ	mass density

SUBSCRIPTS

∞	free-stream conditions
$A, B, C, D, \ldots$	conditions at different points in the flow field
N	conditions on the surface at the vertex of a body
s	conditions immediately behind the shock wave at the vertex of a body

INVISCID FLOW

This study proceeds from the Euler momentum equations,

$$\frac{\partial u}{\partial t}+u\frac{\partial u}{\partial x}+v\frac{\partial u}{\partial y}+w\frac{\partial u}{\partial z}=-\frac{1}{\rho}\frac{\partial p}{\partial x} \tag{1}$$

$$\frac{\partial v}{\partial t}+u\frac{\partial v}{\partial x}+v\frac{\partial v}{\partial y}+w\frac{\partial v}{\partial z}=-\frac{1}{\rho}\frac{\partial p}{\partial y} \tag{2}$$

$$\frac{\partial w}{\partial t}+u\frac{\partial w}{\partial x}+v\frac{\partial w}{\partial y}+w\frac{\partial w}{\partial z}=-\frac{1}{\rho}\frac{\partial p}{\partial z} \tag{3}$$

the continuity equation,

$$\frac{\partial \rho}{\partial t}+\frac{\partial (\rho u)}{\partial x}+\frac{\partial (\rho v)}{\partial y}+\frac{\partial (\rho w)}{\partial z}=0 \tag{4}$$

the equation of state,

$$\rho=\rho\,(p,S) \tag{5}$$

and the energy equation,

$$\frac{\partial S}{\partial t}+u\frac{\partial S}{\partial x}+v\frac{\partial S}{\partial y}+w\frac{\partial S}{\partial z}=0 \tag{6}$$

where u, v, and w are the components of velocity at time t along the X, Y, and Z axes, respectively, of an element of the fluid of density ρ, static pressure p, and entropy S.[2] To put these expressions in a more tractable form, it is convenient to aline the X axis at time t with the direction of the resultant velocity at the origin of the coordinate system. Thus equations (1) through (4) and equation (6) simplify, respectively, in the region of the origin, to

$$\frac{\partial u}{\partial t}+u\frac{\partial u}{\partial x}+\frac{1}{\rho}\frac{\partial p}{\partial x}=0 \tag{7}$$

$$\frac{\partial v}{\partial t}+u\frac{\partial v}{\partial x}+\frac{1}{\rho}\frac{\partial p}{\partial y}=0 \tag{8}$$

$$\frac{\partial w}{\partial t}+u\frac{\partial w}{\partial x}+\frac{1}{\rho}\frac{\partial p}{\partial z}=0 \tag{9}$$

$$\frac{\partial \rho}{\partial t}+u\frac{\partial \rho}{\partial x}+\rho\left(\frac{\partial u}{\partial x}+\frac{\partial v}{\partial y}+\frac{\partial w}{\partial z}\right)=0 \tag{10}$$

and

$$\frac{\partial S}{\partial t}+u\frac{\partial S}{\partial x}=0 \tag{11}$$

which relations are basic to the subsequent analysis.

STEADY FLOW

Characteristics theory.—Compatibility relations describing the behavior of fluid properties along characteristic lines

[2] For certain calculations it may be desirable to proceed from more general equations which include effects of heat and mass addition to (or subtraction from) the flow as well as effects of impressed forces (e. g., gravitational or magnetic). Such a procedure may easily be developed from that presented here by following the method of Guderley (reference 6) for two-dimensional flow.

in supersonic flow may, of course, be obtained by proceeding formally with the theory of characteristics for the quasi-linear partial differential equations which depict the flow. In the interests of simplifying both the derivation of these relations and their resultant forms, however, it seems desirable to proceed in a more intuitive manner, assuming a priori that the pertinent characteristic lines are Mach lines, and utilizing the implication from two-dimensional flow studies that perhaps the most convenient dependent variables are pressure and flow inclination angles.

Now it is clear that in the case of steady flow all derivatives with respect to time disappear from the above relations. Thus, assuming there are no shock waves present in the region of the origin,[3] we may write, with the aid of equations (5) and (11),

$$\frac{\partial \rho}{\partial x}=\frac{\partial \rho}{\partial p}\bigg|_S \frac{\partial p}{\partial x}=\frac{1}{a^2}\frac{\partial p}{\partial x} \tag{12}$$

where a is the local speed of sound in the fluid. Combining equations (7), (10), and (12), there is then obtained the relation

$$\frac{\partial p}{\partial x}=\frac{-\rho u^2}{M^2-1}\left[\frac{1}{u}\left(\frac{\partial v}{\partial y}+\frac{\partial w}{\partial z}\right)\right] \tag{13}$$

or, defining Δ as the angle between the X axis and the tangent to the projection of a streamline in the X-Y plane, and, in an analogous manner, the angle δ in the X-Z plane (see fig. 1), we have

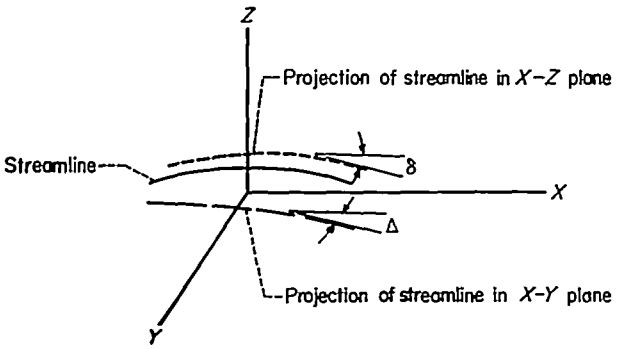

FIGURE 1.—Streamline projections in X-Y and X-Z planes.

$$\frac{\partial p}{\partial x}=\frac{-\rho u^2}{M^2-1}\left(\frac{\partial \Delta}{\partial y}+\frac{\partial \delta}{\partial z}\right) \tag{14}$$

Transforming the derivatives with respect to x and z to derivatives in the characteristic or C_{1z} and C_{2z} directions in the X-Z plane (C_{1z} is positively inclined with respect to X, thus $\partial()/\partial x=[M/(2\sqrt{M^2-1})][\partial()/\partial C_{1z}+\partial()/\partial C_{2z}]$ and $\partial()/\partial z=(M/2)[\partial()/\partial C_{1z}-\partial()/\partial C_{2z}]$) there results from this equation

$$\frac{\partial p}{\partial C_{1z}}+\frac{\partial p}{\partial C_{2z}}=+\frac{\rho u^2}{\sqrt{M^2-1}}\left[\frac{\partial \delta}{\partial C_{2z}}-\frac{\partial \delta}{\partial C_{1z}}-\frac{2}{M}\left(\frac{\partial \Delta}{\partial y}\right)\right] \tag{15}$$

In an analogous manner, there is obtained from equation (9) the relation

$$\frac{\partial p}{\partial C_{1z}}-\frac{\partial p}{\partial C_{2z}}=\frac{-\rho u^2}{\sqrt{M^2-1}}\left(\frac{\partial \delta}{\partial C_{1z}}+\frac{\partial \delta}{\partial C_{2z}}\right) \tag{16}$$

[3] If shock waves are present, the appropriate oblique shock equations are employed.

Adding these two expressions then yields

$$\frac{\partial p}{\partial C_{1z}}=\frac{-\rho u^2}{\sqrt{M^2-1}}\left[\frac{\partial \delta}{\partial C_{1z}}+\frac{1}{M}\left(\frac{\partial \Delta}{\partial y}\right)\right] \tag{17}$$

while subtracting yields

$$\frac{\partial p}{\partial C_{2z}}=\frac{\rho u^2}{\sqrt{M^2-1}}\left[\frac{\partial \delta}{\partial C_{2z}}-\frac{1}{M}\left(\frac{\partial \Delta}{\partial y}\right)\right] \tag{18}$$

Equations (17) and (18) are compatibility equations for characteristic or Mach lines in the X-Z plane.[4] Indeed, if it is further required that the X-Z plane be the osculating plane of the streamline passing through the origin, that is, the plane containing the principal radius of curvature and tangent to this streamline (at the origin), then these equations are the essential relations for determining pressure and flow inclination throughout a flow field. This point becomes evident when it is observed that, with the imposed requirement (viz, $\partial\Delta/\partial x=0$), the additional information derived from studying flow in the X-Y plane is simply that deduced from equation (8), or, as would be expected,

$$\frac{\partial p}{\partial y}=0 \tag{19}$$

In order to construct a flow field, however, it is necessary to know the manner in which the osculating plane rotates and, correspondingly, how the principal curvature varies as we proceed along a streamline. This information is obtained from equations (2) and (3). Differentiation with respect to x yields

$$\frac{\partial^2 \Delta}{\partial x^2}=-\frac{1}{\rho u^2}\frac{\partial}{\partial x}\left(\frac{\partial p}{\partial y}\right)-\frac{\partial \Delta}{\partial z}\frac{\partial \delta}{\partial x} \tag{20}$$

and

$$\frac{\partial^2 \delta}{\partial x^2}=-\frac{1}{\rho u^2}\frac{\partial}{\partial x}\left(\frac{\partial p}{\partial z}\right)-\left(\frac{\partial \delta}{\partial z}+\frac{3}{u}\frac{\partial u}{\partial x}+\frac{1}{\rho a^2}\frac{\partial p}{\partial x}\right)\frac{\partial \delta}{\partial x} \tag{21}$$

respectively.

These and the previously derived expressions form the basis of a characteristics theory for steady three-dimensional flows (see ref. 20). Consistent with the objectives of this paper, however, we are interested in these results as they lead us to a more approximate but, by the same token, a more simplified method of calculating the three-dimensional flow of a gas at high supersonic speeds.

Simplified two-dimensional theory.—It is well at the outset of this analysis to establish, insofar as is practicable, the type of flows to be treated. In this connection, it is convenient to employ the hypersonic similarity parameter (i. e., the product of the flight Mach number and the thickness ratio of a body) as a measuring stick. In flows characterized by values of the hypersonic similarity parameter small compared to 1, that is, flows in which the body is extremely slender and lies close to the axis of the Mach cone, there is no apparent reason to believe that the linear theory will not be as useful an approximate method of calculation

[4] It is noted that these expressions contain not only derivatives in the characteristic directions but also derivatives with respect to the independent variable y. This type of result is to be expected as pointed out by Coburn (ref. 19).

as at low supersonic speeds. In flows characterized by values of the parameter up to about 1, the second-order theory first enunciated by Busemann (ref. 21) for airfoils and more recently generalized to three-dimensional flows by Van Dyke (ref. 9) and Moore (ref. 22) should prove a useful approximation. On the other hand, for flows about more or less arbitrary shapes, there is apparently no approximate method of calculation generally applicable with engineering accuracy at values of the hypersonic similarity parameter appreciably greater than 1.

In the limiting case of indefinitely high free-stream Mach number (and hence similarity parameter) and a ratio of specific heats equal to 1, we have the Newtonian impact theory (ref. 23) and its refined counterpart, accounting for centrifugal forces in the disturbed flow, developed first by Busemann (ref. 24) and more recently treated by Ivey, Klunker, and Bowen (ref. 25). The impact theory has been employed with some success by Grimminger, Williams, and Young (ref. 26) and others to predict surface pressures on bodies of revolution at values of the similarity parameter appreciably greater than 1, although it should be remarked in passing that this success is in part, at least, fortuitous, as perhaps is best evidenced by the fact that the more exact theory (within the framework of the underlying assumption of $M\to\infty$, $\gamma\to 1$) of Busemann is considerably less accurate under corresponding circumstances. As shown in reference 7, neither the Newtonian impact nor the Busemann theory apply with good accuracy to airfoils except at values of the similarity parameter quite large compared to 1, corresponding, for example, in the case of thin airfoils to flight speeds considerably in excess of the escape speed at sea level. Perhaps the foremost shortcoming of these theories is, however, that, irrespective of the shape to which they are applied, they provide no information on the structure [5] of the disturbed flow field which is, of course, of finite extent adjacent to the surface at flight Mach numbers presently of interest (say Mach numbers less than the escape Mach number at sea level). Such information is, for example, important to the determination of the flow about control surfaces and the like which may be located in this field.

In view of the preceding discussion, it seems clear that in the high-supersonic-speed flight regime, a need for an approximate method of analysis lies in the realm of flows characterized by values of the hypersonic similarity parameter greater than 1. An attempt will therefore be made to obtain a method meeting part of this need, attention being focused primarily on flows characterized by large values of the similarity parameter. To this end, it is convenient first to employ equation (14) rewritten in the form

$$\frac{\partial p}{\partial x}=\frac{\rho u^2}{\sqrt{M^2-1}}\left[\frac{\partial\delta}{\partial x}\left(\frac{1-D_z}{1+D_z}\right)-\frac{1}{\sqrt{M^2-1}}\left(\frac{\partial\Delta}{\partial y}\right)\right] \tag{22}$$

where

$$D_z=\frac{\partial\delta/\partial C_{1z}}{\partial\delta/\partial C_{2z}} \tag{23}$$

Now consider for the moment a surface streamline alined in the x direction, and impose the requirement that the X—Z plane be tangent to this streamline and normal to the surface at the point of tangency (the origin). The X—Y plane is then, of course, tangent to the surface at this point. Observing the last term in the brackets on the right-hand side of equation (22), it is noted (see fig. 2) that

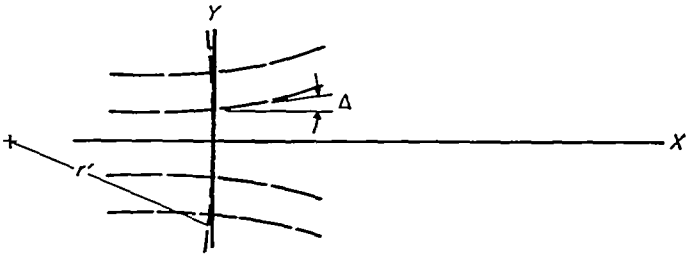

FIGURE 2.—Divergence of streamlines in tangent plane.

$$\frac{\partial\Delta}{\partial y}=\frac{1}{r'}$$

where r' is the radius of curvature of the line normal to the projections of streamlines in the X-Y plane, and passing through the origin. At the high Mach numbers under consideration, the disturbed flow field is confined to a region of small extent normal to the surface of a body; hence it may be expected that r' will be primarily a function of body shape and attitude.[6] This being the case, it follows then that the term $(1/\sqrt{M^2-1})(1/r')$ will decrease in absolute magnitude with increasing Mach number of the flow about the body. Consider now the term $(\partial\delta/\partial x)(1-D_z/(1+D_z)$. We note that $\partial\delta/\partial x=1/R$ where R is the radius of curvature of the projection of a streamline in the X—Z plane and, by reasoning analogous to that used in considering r', is not expected to vary significantly with Mach number in the disturbed flow field. Let us assume for the moment that the quantity $(1-D_z)/(1+D_z)$ is also relatively independent of Mach number. With this assumption, it is clear that equation (22) approaches the equation for two-dimensional flow as the free-stream Mach number, and hence the hypersonic similarity parameter of the flow becomes large compared to 1. The compatibility equations (eqs. (17) and (18)) are affected in a similar manner; thus it is apparent that the flow when viewed in the X—Z plane approaches the two-dimensional type. In this case, however, as shown in reference 7, so long as the Mach number and ratio of specific heats of the disturbed fluid are not too close to 1, D_z is small compared to 1, and hence the flow approaches the generalized Prandtl-Meyer type (i. e., flow in which pressure and inclination angle are approximately constant along curved first-family Mach lines). Our flow equation may then be written

$$\frac{\partial p}{\partial x}\cong\frac{\rho u^2}{\sqrt{M^2-1}}\left(\frac{\partial\delta}{\partial x}\right) \tag{24}$$

where it is required explicitly that

$$\left|\frac{\partial\delta}{\partial x}\right|\gg\frac{1}{\sqrt{M^2-1}}\left|\frac{\partial\Delta}{\partial y}\right| \tag{25}$$

[5] This consequence is traceable primarily to the assumption of $\gamma=1$ which leads to the well-known result that the disturbed flow field is confined to an infinitesimal region adjacent to the surface of a body.

[6] It is interesting to note that in ideal gas flows, r' becomes just-a-function of these variable as the value of the hypersonic similarity parameter becomes large compared to 1 (see work of Oswatitsch, ref. 27, noting that his results can readily be extended to three-dimensional ideal gas flows using the characteristics method of this paper).

or, in effect, that disturbances associated with the divergence of streamlines in tangent planes must be of secondary importance compared to those associated with the curvature of streamlines in planes normal to the surface. Upon closer examination it can easily be deduced that this requirement stems directly from the continuity equation and the condition that it be of the two-dimensional type in the X-Z plane (i. e., $\left|\frac{\partial w}{\partial z}\right| \gg \left|\frac{\partial v}{\partial y}\right|$ in eq. (10)).

From these considerations it appears that the conclusion of reference 10 that inviscid flow along streamlines downstream of the nose of noninclined bodies of revolution traveling at high supersonic speeds may be of the Prandtl-Meyer type (in regions free of shock waves) applies also to other steady three-dimensional flows. It is true, too, that in the latter case, just as in the former case, this conclusion is consistent with the predictions of the hypersonic similarity law for steady flow about slender shapes.

One question remains to be considered, namely, where do the streamlines go in the disturbed flow? To clarify this matter, it is convenient to study further the implications of equation (25). For this purpose we combine equation (25) with the transformation equation

$$\frac{\partial \Delta}{\partial y} = \frac{M}{2}\left(\frac{\partial \Delta}{\partial C_{1y}} - \frac{\partial \Delta}{\partial C_{2y}}\right)$$

to obtain the relation

$$\left|\frac{\partial \delta}{\partial x}\right| \gg \frac{M}{2\sqrt{M^2-1}}\left|\frac{\partial \Delta}{\partial C_{1y}} - \frac{\partial \Delta}{\partial C_{2y}}\right| \tag{26}$$

From this relation we deduce either that to the order of a number (curvature) small compared to $\frac{2\sqrt{M^2-1}}{M}\left|\frac{\partial \delta}{\partial x}\right|$

$$\frac{\partial \Delta}{\partial C_{1y}} \cong \frac{\partial \Delta}{\partial C_{2y}} \tag{27}$$

or that

$$\left.\begin{aligned} \left|\frac{\partial \delta}{\partial x}\right| &\gg \frac{M}{2\sqrt{M^2-1}}\left|\frac{\partial \Delta}{\partial C_{1y}}\right| \\ \text{and} \qquad \left|\frac{\partial \delta}{\partial x}\right| &\gg \frac{M}{2\sqrt{M^2-1}}\left|\frac{\partial \Delta}{\partial C_{2y}}\right| \end{aligned}\right\} \tag{28}$$

Equation (27) implies vortical flow, however, which type of flow cannot be treated by the present analysis since equation (25) is violated.[7] Equation (28) is then the requirement consistent with the basic assumptions of this analysis. Comparing the relations of equation (28) with the transformation equation

$$\frac{\partial \Delta}{\partial x} = \frac{M}{2\sqrt{M^2-1}}\left(\frac{\partial \Delta}{\partial C_{1y}} + \frac{\partial \Delta}{\partial C_{2y}}\right)$$

leads one to the conclusion, however, that

$$\left|\frac{\partial \delta}{\partial x}\right| \gg \left|\frac{\partial \Delta}{\partial x}\right| \tag{29}$$

or, in effect, that consistent with equation (25) geodesic lines can be treated as surface streamlines. With this information we are enabled to construct the flow field about a body, having once determined, for example, the flow in the region of the leading edge (or edges) thereof. This result follows since a geodesic line, and hence a streamline, on the surface is fixed, provided its direction at any point is given (see, e.g., ref. 28).[8] With this knowledge of the location of surface streamlines, flow in the planes tangent thereto and normal to the surface may be calculated approximately in the relatively thin region between the surface and bounding shock waves, using the generalized shock-expansion method in the manner described in reference 7.

A partial check on these observations is afforded by studying the flow about a swept airfoil. In this case flow at the surface may be calculated with good accuracy, using the shock-expansion method in combination with simple-sweep theory. For thin airfoils (on the surfaces of which the appropriate geodesics have essentially the direction of the free stream) the generalized shock-expansion method of this paper reduces to the slender-airfoil method of reference 7. Thus, in this case, it is evident from the results of reference 7 that the generalized method will predict surface pressure coefficients in error by less than 10 percent, providing the component of free-stream Mach number normal to the leading edge is greater than about 3. It is of interest also to consider a thick airfoil to ascertain the accuracy with which this method applies to flow with appreciable curvature. To this end, surface pressure coefficients and streamlines have been calculated for a 20-percent-thick biconvex airfoil (at zero incidence) swept 60° and operating at Mach numbers of 10 and infinity ($\gamma=1.4$). Conditions at the leading edge were determined from exact shock-wave relations for both methods. The results of these calculations are presented in figure 3, and it is observed that the pressure distributions determined with the shock-expansion method for swept airfoils and the generalized shock-expansion method are in reasonably good agreement at both Mach numbers. The streamlines are also in reasonably good agreement over the forward portion of the airfoil, although, as would be expected, somewhat poorer results are obtained over the afterportion. It is not surprising, in view of the underlying assumptions of the generalized shock-expansion method, that it is generally more accurate at the highest Mach number.

In the preceding discussion circumstances were deduced under which steady flow at high supersonic speeds about three-dimensional shapes could be constructed approximately, using the basic tools of two-dimensional supersonic flow analysis, namely, the oblique shock equations of Rankine and Hugoniot and the corner expansion equations of Prandtl and Meyer. Several possible exceptions to these circumstances immediately come to mind. These include conical-type flows and flow in the region of the tip of a wing, or at the discontinuous juncture of a wing and body, to mention a few. In such flows equation (25) may not be satisfied, in which case two-dimensional flow in planes

[7] This conclusion is particularly evident in the case of pure vortical flow, or say vortical flow with a superimposed uniform stream directed along the axis of the vorter, in which cases $\frac{\partial p}{\partial x}=0$, and hence equation (24) certainly does not follow from equation (22).

[8] If a sudden change of surface slope causes an oblique shock wave or a concentrated Prandtl-Meyer type expansion fan, the streamlines in the downstream direction are defined on the basis of their flow direction immediately following the discontinuity in slope.

normal to a surface cannot be expected.[9] It might be reasoned, therefore, that these flows cannot, in general, be treated by the proposed method. This observation may be correct; however, in one case investigated thus far in this connection, namely, flow in the region of the nose of nonlifting bodies of revolution (see ref. 10), it was found that although equation (25) is not satisfied, flow along streamlines is nevertheless of approximately the Prandtl-Meyer type. Thus we are led to expect that perhaps a less restrictive requirement than the satisfying of equation (25) may be imposed to insure that flow along streamlines is of this type. Such a requirement is in fact easily obtained by reconsidering equation (22) in the form

$$\frac{\partial p}{\partial x}=\frac{\rho u^2}{\sqrt{M^2-1}}\left[\frac{\partial \delta}{\partial x}-\frac{M}{\sqrt{M^2-1}}\left(\frac{\partial \delta}{\partial C_{l_x}}+\frac{1}{M}\frac{\partial \Delta}{\partial y}\right)\right] \tag{30}$$

thus yielding

$$\left|\frac{\partial \delta}{\partial x}\right| \gg \frac{M}{\sqrt{M^2-1}}\left|\frac{\partial \delta}{\partial C_{l_x}}+\frac{1}{M}\frac{\partial \Delta}{\partial y}\right| \tag{31}$$

It is evident that equation (31) embraces equation (25) as a special case and that Prandtl-Meyer flow obtains along streamlines if

$$\frac{\partial \delta}{\partial C_{l_x}} \cong -\frac{1}{M}\frac{\partial \Delta}{\partial y} \tag{32}$$

to the order of a number small compared to $\frac{\sqrt{M^2-1}}{M}\left|\frac{\partial \delta}{\partial x}\right|$. This result implies that although flow inclination angles are not necessarily constant along C_{l_x} lines, pressure is approximately constant (see eq. (17)).

[9] One may note that in some cases of this nature, the flow in osculating planes of the streamlines may be of the two-dimensional or even the simpler Prandtl-Meyer type, although these planes may not be normal to the surface.

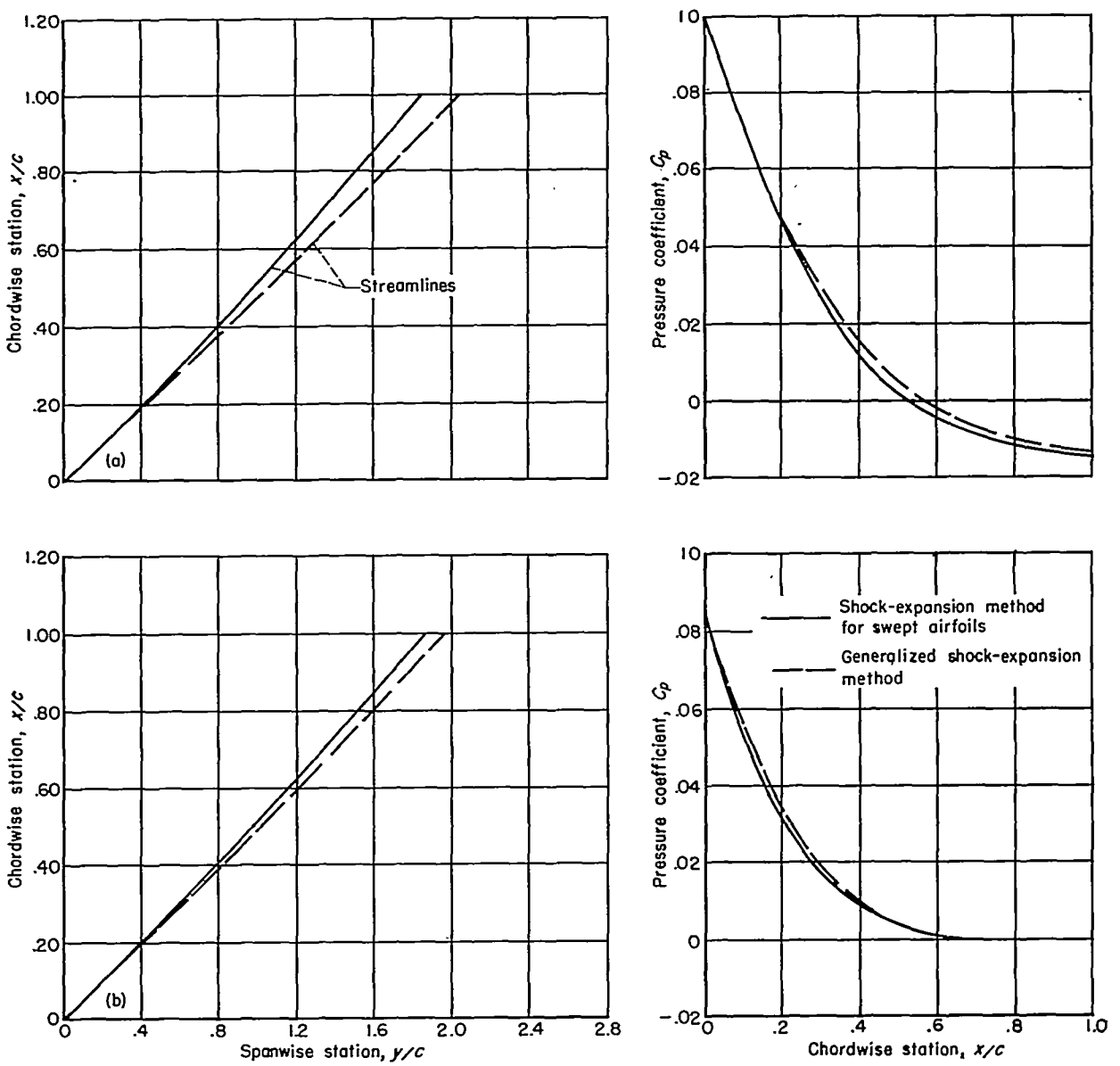

(a) $M_\infty = 10$
(b) $M_\infty = \infty$

FIGURE 3.—Comparison of surface streamlines and pressure distributions calculated with the generalized shock-expansion method and the shock-expansion method for swept airfoils (biconvex airfoil section, thickness ratio=0.2, sweep angle=60°).

It is clear that the increased generality of the above result has been obtained at some expense in our knowledge of the streamline flow pattern. For example, it is not now indicated that (within the framework of this analysis) surface streamlines may generally be taken as geodesics—additional knowledge of the flow must be had in order to determine these streamlines. If they are known, however, the calculation of the whole flow field is materially facilitated by the above considerations.

Thus far only steady flows have been considered. The next problem is to extend these considerations to nonsteady flows and some aspects of this matter will now be discussed.

NONSTEADY FLOW

The methods of analysis in this case are entirely analogous to those employed in the study of steady flow, the singular contrasting feature being that derivatives with respect to time in equations (1) through (11) cannot now be neglected. With this point in mind, only pertinent results are discussed below.

Characteristics theory.—The compatibility equations relating fluid properties along Mach lines may be written as follows:

$$\frac{\partial p}{\partial C_{1z}}=\frac{-\rho u^2}{\sqrt{M^2-1}}\left\{\frac{\partial \delta}{\partial C_{1z}}+\frac{1}{M}\left(\frac{\partial \Delta}{\partial y}\right)+\frac{1}{u}\left[\frac{\sqrt{M^2-1}}{M}\left(\frac{\partial \delta}{\partial t}\right)+\frac{M}{\rho u^2}\left(\frac{\partial p}{\partial t}\right)-\frac{1}{Mu}\left(\frac{\partial u}{\partial t}\right)\right]\right\} \tag{33}$$

and

$$\frac{\partial p}{\partial C_{2z}}=\frac{+\rho u^2}{\sqrt{M^2-1}}\left\{\frac{\partial \delta}{\partial C_{2z}}-\frac{1}{M}\left(\frac{\partial \Delta}{\partial y}\right)+\frac{1}{u}\left[\frac{\sqrt{M^2-1}}{M}\left(\frac{\partial \delta}{\partial t}\right)-\frac{M}{\rho u^2}\left(\frac{\partial p}{\partial t}\right)+\frac{1}{Mu}\left(\frac{\partial u}{\partial t}\right)\right]\right\} \tag{34}$$

The definition of the X-Z plane as the osculating plane of a pathline (streamline in steady flow) remains as before, hence equation (19) still applies in the X-Y plane in the region of the origin. The rotation of the osculating plane and variation of the principal curvature of a pathline with motion along it are now, however, obtained with the aid of the relations

$$\frac{d^2\Delta}{dx^2}=-\frac{1}{\rho u^2}\frac{d}{dx}\left(\frac{\partial p}{\partial y}\right)-\frac{\partial \Delta}{\partial z}\left(\frac{d\delta}{dx}\right) \tag{35}$$

and

$$\frac{d^2\delta}{dx^2}=-\frac{1}{\rho u^2}\frac{d}{dx}\left(\frac{\partial p}{\partial z}\right)-\left(\frac{\partial \delta}{\partial z}+\frac{3}{u}\frac{du}{dx}+\frac{1}{\rho a^2}\frac{dp}{dx}\right)\frac{d\delta}{dx} \tag{36}$$

where

$$\frac{d}{dx}=\frac{\partial}{\partial x}+\frac{1}{u}\left(\frac{\partial}{\partial t}\right) \tag{37}$$

These equations are basic to characteristics theory in its application to three-dimensional nonsteady flows (see ref. 20). However, as in the case of steady flows, they can best be employed for our purposes to obtain a simplified method of calculation.

Simplified two-dimensional theory.—It is recalled that the essential simplification in our treatment of three-dimensional steady flows derived from the fact that they often appear locally two-dimensional and hence they can be treated with the generalized shock-expansion method of reference 7. In the following study of nonsteady flows we will profit from this experience by anticipating that the desired simplified theory is again this shock-expansion method. Accordingly, our problem is reduced to that of determining the conditions under which the method can be applied to the calculation of nonsteady hypersonic flows.

One condition is, for all practical purposes, self-evident; namely, the local Mach number of the disturbed flow must be everywhere large compared to 1. This requirement must manifest itself since, otherwise, nonsteady disturbances created an appreciable distance upstream and/or downstream of a particle could significantly influence its behavior in the disturbed flow field (see fig. 4, noting that in case of thick body, particle b is influenced by disturbances originating in particles a and c) and this situation would preclude the possibility of Prandtl-Meyer type flow along pathlines. It follows then that the shock-expansion method can be applied only to thin or slender shapes (i. e., shapes producing flow deflections small compared to 1) at hypersonic speeds.

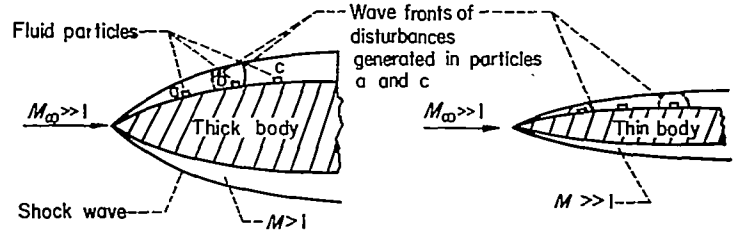

FIGURE 4.—Propagation of nonsteady disturbances in flow about thick and thin bodies.

With this requirement in mind it is convenient to rewrite the compatibility equations (33) and (34) in the form they assume when $M \gg 1$. Thus with slight rearranging we have

$$\frac{\partial p}{\partial C_{1z}}+\frac{1}{u}\frac{\partial p}{\partial t}=\frac{-\rho u^2}{M}\left(\frac{\partial \delta}{\partial C_{1z}}+\frac{1}{u}\frac{\partial \delta}{\partial t}+\frac{1}{M}\frac{\partial \Delta}{\partial y}-\frac{1}{Mu^2}\frac{\partial u}{\partial t}\right)$$

and

$$\frac{\partial p}{\partial C_{2z}}+\frac{1}{u}\frac{\partial p}{\partial t}=\frac{\rho u^2}{M}\left(\frac{\partial \delta}{\partial C_{2z}}+\frac{1}{u}\frac{\partial \delta}{\partial t}-\frac{1}{M}\frac{\partial \Delta}{\partial y}+\frac{1}{Mu^2}\frac{\partial u}{\partial t}\right)$$

Now, consistent with the requirement $M \gg 1$, the term $(1/Mu^2)(\partial u/\partial t)$ on the right in these equations can be neglected by comparison to the other terms. If, in addition, we define (after eq. (37)) the derivatives

$$\frac{d}{dC_{1z}}=\frac{\partial}{\partial C_{1z}}+\frac{1}{u}\left(\frac{\partial}{\partial t}\right)$$

and

$$\frac{d}{dC_{2z}}=\frac{\partial}{\partial C_{2z}}+\frac{1}{u}\left(\frac{\partial}{\partial t}\right)$$

and note that now

$$\frac{d}{dx}=\frac{1}{2}\left(\frac{d}{dC_{1z}}+\frac{d}{dC_{2z}}\right)$$

then these equations can be combined to yield the pressure gradient along a pathline in the following form

$$\frac{dp}{dx}=\frac{\rho u^2}{M}\left[\frac{d\delta}{dx}\left(\frac{1-\frac{d\delta/dC_{1x}}{d\delta/dC_{2x}}}{1+\frac{d\delta/dC_{1x}}{d\delta/dC_{2x}}}\right)-\frac{1}{M}\frac{\partial\Delta}{\partial y}\right] \tag{38}$$

But $\frac{d\delta/dC_{1x}}{d\delta/dC_{2x}}$ is analagous to D_x in steady flow; that is, in the event the term $(1/M)\ (\partial\Delta/\partial y)$ is negligible in this expression, $\frac{d\delta/dC_{1x}}{d\delta/dC_{2x}}$ may be identified with disturbances reflected from shock waves in the flow. Just as in the case of steady flow (see ref. 7), however, these reflected disturbances are of very small strength by comparison to the incident disturbances when $M\gg1$ and so $\frac{d\delta/dC_{1x}}{d\delta/dC_{2x}}$ must be small compared to 1. Provided, then, that

$$\left.\begin{aligned} &M\gg1\\ &\left|\frac{d\delta}{dx}\right|\gg\frac{1}{M}\left|\frac{\partial\Delta}{\partial y}\right| \end{aligned}\right\} \tag{39}$$

equation (38) may be written [10]

$$\frac{dp}{dx}=\frac{\rho u^2}{M}\frac{d\delta}{dx} \tag{40}$$

which result implies, of course, Prandtl-Meyer flow along pathlines. It follows that equations (39) are sufficient conditions under which the generalized shock-expansion method can be used to calculate nonsteady hypersonic flows.

When these conditions are satisfied, we note, by analogy to the steady flow case, that pathlines in the surfaces swept out by elements of fluid adjacent to shapes in nonsteady motion are approximated by geodesics or, even simpler, lines of curvature of these surfaces. It is not to be implied, of course, that pathlines must always be such curves in order for fluid properties to behave as in Prandtl-Meyer flow. In fact, again, just as in the case of steady flow, if the condition $\left|\frac{d\delta}{dx}\right|\gg\left|\frac{d\delta}{dC_{1x}}+\frac{1}{M}\frac{\partial\Delta}{\partial y}\right|$ is satisfied rather than the second of equations (39), pathlines are not necessarily geodesics (or lines of curvature) even though the first of equations (39) and hence equation (40) holds along these lines.

One notes that within the framework of this approximate analysis, the calculation of nonsteady flows at the surface of slender bodies traveling at high supersonic speeds should not prove unduly difficult. To illustrate, consider an oscillating airfoil as shown in figure 5. The pressure at any point along the pathline shown is readily deduced by simply integrating equation (40) along this line from the leading edge of the airfoil to the point in question. The whole flow field as a function of time may be calculated by employing the generalized shock-expansion method for steady flows (see ref. 7) in a series of planes located small distances apart in time. This example serves to emphasize that, in general, the time history of fluid elements must be known, at least to the extent of fixing their initial flow direction and entropy.[11] It is also evident that again, as in the case of steady flow, the general results of the analysis are consistent with the predictions of the hypersonic similarity law for nonsteady flows about slender related shapes (ref. 5).

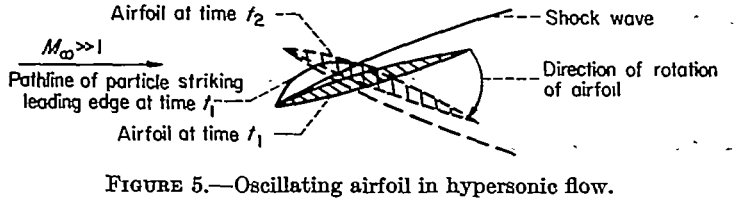

FIGURE 5.—Oscillating airfoil in hypersonic flow.

These considerations complete our general treatment of inviscid hypersonic flows. It is appropriate to turn next to effects of viscosity as they relate to the hypersonic boundary layer.

VISCOUS FLOW—THE HYPERSONIC BOUNDARY LAYER

The arguments presented here are concerned with the steady hypersonic boundary layer, and they will be, for the most part, physical.[12] Furthermore, they will appear as natural extensions of conclusions reached in our study of inviscid hypersonic flow. Let us reconsider, then, the motion of the inviscid fluid. We have established that this motion is, under certain well-defined circumstances, confined locally to planes normal to the surface of a body and tangent to surface streamlines. Correspondingly, there is no sensible momentum transfer across these planes. Now if viscous forces are set up in the flow bounding the surface, we recognize that they will act to resist the motion of the fluid—that is, the motion in the normal planes. Evidently, then, these forces act in the same planes of local two-dimensional flow as the pressure forces, and it must follow, of course, that resultant changes in momentum of the fluid also occur in these planes.

Consider now the changes in energy of the disturbed fluid. These changes can be brought about by viscous or dissipative work, pressure work, heat convection, and heat conduction.[13] It was just found, however, that the forces doing work act in the normal planes; hence we conclude that the corresponding changes in energy occur in these planes. Similarly, heat is convected in the normal planes, since mass is convected in these planes. Finally, we conclude also that heat is conducted locally in the normal planes inasmuch as the temperature gradients set up by the action of viscous forces are confined primarily to these planes.[14] Evidently, then, changes in energy of the fluid can be treated locally as a two-dimensional phenomenon in planes normal to the surface of a body.

[10] The derivation of equation (40) presented here has the virtue of being both more complete and more general than the corresponding derivation of reference 20.

[11] In the special case of slender airfoils for which the hypersonic similarity parameter of the flow is less than 1, entropy gradients in the disturbed flow can frequently be neglected, with the advantage of relaxing these two conditions and thus substantially simplifying the problem (see, e. g., ref. 29).

[12] Although not presented, corresponding mathematical arguments have been pursued using the Navier-Stokes and energy equations, and the final results confirm those obtained here. It is indicated, too, that these results may apply also to nonsteady boundary-layer flows.

[13] Radiation and absorption may, of course, also contribute to the energy changes; however, it is beyond the scope of this paper to consider these phenomena.

[14] One might conceive of severe temperature gradients being imposed at the wall boundary by, for example, extremely nonuniform surface cooling. Such gradients, if transverse to streamlines, would naturally invalidate this argument.

Thus far we have been concerned mainly with forces and their relation to the momentum and energy of the fluid. The question of conserving mass remains to be investigated. It will be recalled that the requirement of conservation of mass was the essential factor which determined when the generalized shock-expansion method could be employed to calculate three-dimensional flows. This requirement is physically (and mathematically) the same, independent of whether or not viscous forces come into play. We conclude then that for the purposes of this study, equation (25) can be used to determine when the three-dimensional boundary layer can be calculated with two-dimensional equations. From equation (25) it is indicated that the boundary layer must be largely hypersonic if this calculation is to be permissible. It is not to be implied, however, that the boundary layer always becomes two-dimensional, as on an airfoil, if the stream Mach number is made extremely large. For example, in the case of axial flow about the right circular cone, equation (25) is violated independent of Mach number (just as with inviscid flow) and we must use something like the Mangler transformation (ref. 30) in the boundary-layer calculations. On the other hand, if the body, instead of being conical, is curved in the stream direction, then it is indicated that the boundary-layer flow should approach the two-dimensional type with increasing Mach number.

This discussion completes our arguments regarding the two-dimensionality of three-dimensional hypersonic flows. Attention is turned next to a practical application of this concept.

APPLICATION OF THEORY TO BODIES OF REVOLUTION IN STEADY FLIGHT

The critical feature of this application is the analysis of the inviscid flow, since known two-dimensional boundary-layer solutions can be readily employed once this flow is known. Accordingly, the following discussion is restricted to the inviscid flow problem.

Now it was shown previously in this paper that a large class of hypersonic flows which are basically three-dimensional can be calculated with a generalized shock-expansion method which is analogous to that employed in reference 7 for studying flow about airfoils. Specifically, this treatment is permissible when disturbances associated with the divergence of streamlines in planes tangent to a surface can be considered negligible compared to those associated with the curvature of streamlines in planes normal to the surface (see eq. (25)). For the case of noninclined bodies of revolution which are curved in the stream direction, this requirement is satisfied when the hypersonic similarity parameter K is greater than about 1 (see ref. 10). For inclined bodies, an additional restriction is imposed. This point is perhaps best clarified by considering the problem of calculating flow at the surface.

FLOW AT THE SURFACE

It follows from the inviscid flow analysis that when the generalized shock-expansion method applies in the region downstream of the vertex, surface streamlines can be approximated by geodesic lines. The only geodesics on the surface of a body of revolution which, like streamlines, do not intersect each other are the meridian lines. In addition, the meridian lines are the only geodesics which, like the streamlines, pass through the vertex. When the shock-expansion method is applied, then, surface streamlines are approximated by meridian lines. Strictly speaking, however, this approximation is valid only in the case of $\alpha \ll 1$. (It is, of course, always true, independent of α on the extreme windward and leeward sides of a body.) Evidently, then, the generalized shock-expansion method should be applicable to curved bodies of revolution only at small angles of attack in flows characterized by a value of the hypersonic similarity parameter greater than about 1.

The procedure for determining flow conditions at the surface of a lifting body is entirely analogous to that employed in the application of the shock-expansion method to the nonlifting body (ref. 10). Thus, it is assumed that the flow at the vertex is the same as that for a cone tangent to the body at this point and, hence, may be determined from existing conical-flow theory (see, e. g., ref. 31 for moderate supersonic Mach numbers and ref. 32 for high supersonic Mach numbers). More specifically, the Mach number at the vertex under the vortical layer [15] may be calculated by means of the pertinent conical-flow expressions in reference 31 or reference 32. The variation of Mach number downstream of the vertex is then obtained by means of the Prandtl-Meyer angle ν (see, e. g., ref. 33) which in turn is determined from the isentropic expansion relation

$$\delta_A+\nu_A=\delta_B+\nu_B \tag{41}$$

where A and B are different points on the same meridian line. Since the flow is isentropic in the windward plane of symmetry downstream of the shock at the vertex and around the surface of the body, the pressure distribution (in coefficient form) is readily obtainable with the aid of the expression

$$C_p=\frac{2}{\gamma M_\infty^2}\left(\frac{p_s}{p_\infty}\frac{p}{p_s}-1\right) \tag{42}$$

where p_s/p_∞ is the pressure rise across the shock at the vertex on the windward side of the body and is determined from conical-flow theory. The ratio p/p_s is given by

$$\frac{p}{p_s}=\left(\frac{1+\frac{\gamma-1}{2}M_s^2}{1+\frac{\gamma-1}{2}M^2}\right)^{\frac{\gamma}{\gamma-1}} \tag{43}$$

where M is known from equation (41) and M_s is the Mach number immediately downstream of the shock on the windward side of the body at the vertex and, hence, is also determined from conical-flow theory.

FLOW OFF THE SURFACE

Flow in meridian planes around bodies of revolution may be calculated by the generalized shock-expansion method in much the same manner as the procedure employed in reference 7 for flow about airfoils. However, the application of the method is somewhat more complicated for the case of a

[15] Since a vortical layer exists around the body surface at the vertex (see, e. g., ref. 13) a vortical layer must also exist downstream of the vertex.

body of revolution since now the influence of the conical-flow region at the vertex must be considered. An analysis for flow in the region of the vertex of a nonlifting body of revolution ($K>1$) was presented in reference 34 and expressions were developed which yield the shock-wave curvature as well as flow conditions along a line (normal to the body axis) a short distance downstream of the vertex. This analysis was extended to lifting bodies and more general expressions were presented in reference 32. Thus, initial conditions in the region of the vertex can be established. There remains the determination of flow conditions along meridian lines downstream of the vertex externally adjacent to the vortical layer. These conditions may be determined in the same manner as for flow directly on the surface (i. e., under the vortical layer), except that now initial flow conditions externally adjacent to the vortical layer at the vertex are employed in the isentropic expansion relations. Construction of the flow field between the shock and the vortical layer in each meridian plane can then proceed in a manner analogous to that for the two-dimensional airfoil discussed in reference 7. To illustrate, consider the flow in a meridian plane of a lifting body of revolution (see fig. 6).

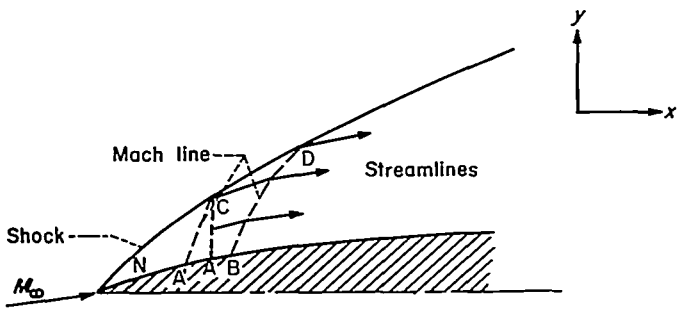

FIGURE 6.—Schematic diagram of flow field about a body of revolution.

All fluid properties at points N, A′, A, B and so forth, on the body surface external to the vortical layer are calculated with the aid of the oblique shock-wave, conical-flow, and expansion equations. Flow conditions along the line AC may then be determined (see ref. 32). It will be recalled (see ref. 7) that a basic condition employed in constructing flow fields about airfoils by the generalized shock-expansion method is that the pressure is constant along Mach lines emanating from the surface. In the case of flow about pointed bodies of revolution, this condition can be relaxed to account for the small variations in pressure due to the influence of the conical type flow in the region of the vertex. The procedure is as follows. The Mach line A′C is constructed using the known conditions in the region NAC shown in the sketch. The net pressure change along this Mach line (i. e., $p_C - p_{A'}$) is thus determined. This pressure difference is then assumed to represent the net pressure change between the body surface and the shock along each Mach line emanating from the surface downstream of the vertex. The flow field is constructed using this criteria in conjunction with the isentropic expansion relations for flow along stream lines.

FORCES AND MOMENTS ACTING ON BODIES OF REVOLUTION

It is of interest now to consider briefly the forces acting on a body of revolution. In the previous discussion, attention was called to the fact that the flow is isentropic in the windward plane of symmetry at the vertex as well as on the surface of the body. This result materially reduces the net labor associated with carrying out the calculations to determine the pressure distributions around the body downstream of the vertex since the pressure rise, as well as the change in entropy through the shock, need be considered only in this plane at the vertex. The normal-force, axial-force, and pitching-moment coefficients may be obtained from the expressions

$$C_N=\frac{16}{\gamma M_\infty^2 \pi d^2}\int_0^l\int_0^r \frac{p}{p_\infty} r\cos\varphi\, d\varphi\, dx \tag{44}$$

$$C_A=\frac{16}{\gamma M_\infty^2 \pi d^2}\int_0^l\int_0^r r\tan\delta\left(\frac{p}{p_\infty}-1\right) d\varphi\, dx \tag{45}$$

$$C_m=\frac{16}{\gamma M_\infty^2 \pi d^2 l}\int_0^l\int_0^r \frac{p}{p_\infty} rx\cos\varphi\, d\varphi\, dx \tag{46}$$

respectively, where d is the diameter of the base, r is the radius of the body, φ is the meridian angle measured from the plane of symmetry on the windward side of the body, and x is measured along the body axis. If equations (44) and (46) are differentiated with respect to α and the condition of constant entropy on the surface is employed, there is obtained

$$(C_{N_\alpha})_{\alpha=0}=\frac{16}{\gamma M_\infty^2 \pi d^2}\int_0^l\int_0^r \frac{p}{p_N}\frac{\sin 2\mu_N}{\sin 2\mu}\frac{\partial}{\partial\alpha}\left(\frac{p_N}{p_\infty}\right) r\cos\varphi\, d\varphi\, dx \tag{47}$$

and

$$(C_{m_\alpha})_{\alpha=0}=\frac{16}{\gamma M_\infty^2 \pi d^2 l}\int_0^l\int_0^r \frac{p}{p_N}\frac{\sin 2\mu_N}{\sin 2\mu}\frac{\partial}{\partial\alpha}\left(\frac{p_N}{p_\infty}\right) rx\cos\varphi\, d\varphi\, dx \tag{48}$$

These expressions define the initial slopes of the normal-force- and pitching-moment-coefficient curves, respectively, and may be rewritten in terms of the initial normal-force-curve slope for a cone tangent to the body at the vertex; thus,

$$(C_{N_\alpha})_{\alpha=0}=8\left(\frac{l}{d}\right)^2\tan\delta_N\,(C_{N_\alpha})_{TCN}\int_0^1 \frac{p}{p_N}\frac{\sin 2\mu_N}{\sin 2\mu}\left(\frac{r}{l}\right) d\left(\frac{x}{l}\right) \tag{49}$$

and

$$(C_{m_\alpha})_{\alpha=0}=8\left(\frac{l}{d}\right)^2\tan\delta_N\,(C_{N_\alpha})_{TCN}\int_0^1 \frac{p}{p_N}\frac{\sin 2\mu_N}{\sin 2\mu}\left(\frac{r}{l}\right)\left(\frac{x}{l}\right) d\left(\frac{x}{l}\right) \tag{50}$$

where the subscript TCN refers to a cone tangent at the vertex. The calculations necessary to determine the initial normal-force- and pitching-moment-curve slopes for a body of revolution are then relatively simple, since $(C_{N_\alpha})_{TCN}$ may be easily obtained from reference 12 or from chart 8 in

reference 33. The Mach number and pressure distributions along the body are obtained by the shock-expansion method for the case $\alpha=0$. When these distributions have been determined, the integral terms in equations (49) and (50) are easily evaluated by numerical integration or by graphical methods.

SIMPLIFIED EXPRESSIONS FOR SLENDER BODIES

In the case of slender bodies traveling at very high supersonic Mach numbers and very small angles of attack the calculations of fluid properties at the surface become relatively simple. In fact, fluid properties downstream of the vertex may be related to those at the vertex by means of explicit algebraic expressions. In particular, the local Mach number and pressure distributions on the surface of a slender body may be written (see ref. 32)

$$M=\frac{M_N}{1-\frac{\gamma-1}{2}(M_N\delta_N)\left(1-\frac{\delta}{\delta_N}\right)} \tag{51}$$

and

$$C_p=\frac{2}{\gamma M_\infty^2}\left\{\left(\frac{p_s}{p_\infty}\right)_{\varphi=0}\left[\frac{(M_s)_{\varphi=0}}{M_N}-\frac{\gamma-1}{2}(M_s\delta_N)_{\varphi=0}\left(1-\frac{\delta}{\delta_N}\right)\right]^{\frac{2\gamma}{\gamma-1}}-1\right\} \tag{52}$$

respectively, where δ is measured relative to the body axis in these and subsequent expressions. Equations (51) and (52) combine with the corresponding conical-flow equations (ref. 32) to predict the ratios of local to free-stream Mach numbers and local to free-stream static pressures to be the same at corresponding points on related bodies, provided the flow fields about these bodies are defined by the same respective values of the hypersonic similarity parameters $M_\infty\delta_N$ and $M_\infty\alpha$ (or α/δ_N). These predictions are in agreement with those of reference 3 for inviscid flow about slender three-dimensional shapes, and they enable the solution of equations (51) and (52) in terms of tabulated functions of the similarity parameters. Calculations over a range of $M_\infty\delta_N$ from 0.60 to ∞ and α/δ_N from 0 to 1 were carried out for flow at the vertex of a body of revolution[16] and the results of these calculations for the flow parameters $\frac{(M_s)_{\varphi=0}}{M_N}$, $\frac{(p_s/p_\infty)_{\varphi=0}}{(M_\infty\delta_N)^2}$, and $(M_s\delta_N)_{\varphi=0}$ are tabulated in table I for 30° increments of φ from 0 to π. For a given $M_\infty\delta_N$ and $M_\infty\alpha$, the Mach number on the surface of a body downstream of the vertex is readily obtained with the aid of these tabulated parameters when used in conjunction with equation (51). The pressure coefficient is easily calculated by means of equation (52).

The results from table I may also be used to good advantage in determining the initial slopes of the normal-force- and pitching-moment-coefficient curves for slender bodies.[17] For example, when $M>>1$ and $\delta<<1$, equations (49) and (50) combine with equations (51) and (52) to yield

$$(C_{N_\alpha})_{\alpha=0}=8\left(\frac{l}{d}\right)^2\delta_N\,(C_{N_\alpha})_{TCN}\int_0^1\left[1-\frac{\gamma-1}{2}(M_N\delta_N)\left(1-\frac{\delta}{\delta_N}\right)\right]^{\frac{\gamma+1}{\gamma-1}}\left(\frac{r}{l}\right)d\left(\frac{x}{l}\right) \tag{53}$$

and

$$(C_{m_\alpha})_{\alpha=0}=8\left(\frac{l}{d}\right)^2\delta_N\,(C_{N_\alpha})_{TCN}\int_0^1\left[1-\frac{\gamma-1}{2}(M_N\delta_N)\left(1-\frac{\delta}{\delta_N}\right)\right]^{\frac{\gamma+1}{\gamma-1}}\left(\frac{r}{l}\right)\left(\frac{x}{l}\right)d\left(\frac{x}{l}\right) \tag{54}$$

respectively, where

$$(C_{N_\alpha})_{TCN}=\frac{\left(\frac{M_s}{M_N}\right)^{\frac{2\gamma}{\gamma-1}}\left[1+\frac{\gamma+3}{2}(M_\infty\delta_N)^2\right]\left\{\left[1+\frac{\gamma-1}{2}(M_\infty\delta_N)^2\right]\left[1+\gamma\,(M_\infty\delta_N)^2\right]\left(\frac{M_N}{M_\infty}\right)^2-\left(\frac{\delta_s}{\delta_N}\right)^2(M_\infty\delta_N)^2\right\}}{(M_\infty\delta_N)^2\left[\frac{\gamma+5}{\gamma+1}\left(\frac{\delta_N}{\delta_s}\right)-1\right]\left[1+\frac{\gamma-1}{2}(M_\infty\delta_N)^2\right]} \tag{55}$$

These expressions are easily evaluated with the aid of the tabulated flow parameters in table I for the case $\alpha/\delta_N=0$.

EXPERIMENT

In order to obtain a check on the predictions of the preceding theoretical analysis, the pressures acting on the surfaces of bodies of revolution corresponding to values of the hypersonic similarity parameter K from 0.60 to 2.1 at Mach numbers from 3.00 to 6.30 were determined experimentally. The bodies were tested at angles of attack up to 15°. A brief description of these tests follows.

TEST APPARATUS

Tests were conducted in the Ames 10- by 14-inch supersonic wind tunnel. A detailed description of the wind tunnel and auxiliary equipment may be found in reference 35.

The pressures acting on the model surfaces were measured with a mercury U-tube manometer or by means of McLeod gages when the pressures were low enough to be recorded on the latter.

Pressure-distribution models were mounted on a 0° model support and on 5°, 10°, and 15° bent supports. The test models were two tangent ogives having fineness ratios 3 and 5 and two cones having the same vertex angles as the ogives. The dimensions of these models and location of the pressure orifices are shown in figure 7.

[16] The conical flow expressions presented in reference 32 were employed in these calculations. It will be noted in table I that the value of $\frac{(M_s)_{\varphi=0}}{M_N}$ is not given for all values of φ. This results from the fact that as $\alpha\to\delta_N$ and $M_\infty\delta_N\to\infty$, the assumption of an infinitesimally thin vortical layer is violated and, hence, the slender-cone theory yields unrealistic results for these conditions.

[17] The initial axial-force-curve slope is, of course, zero due to symmetry.

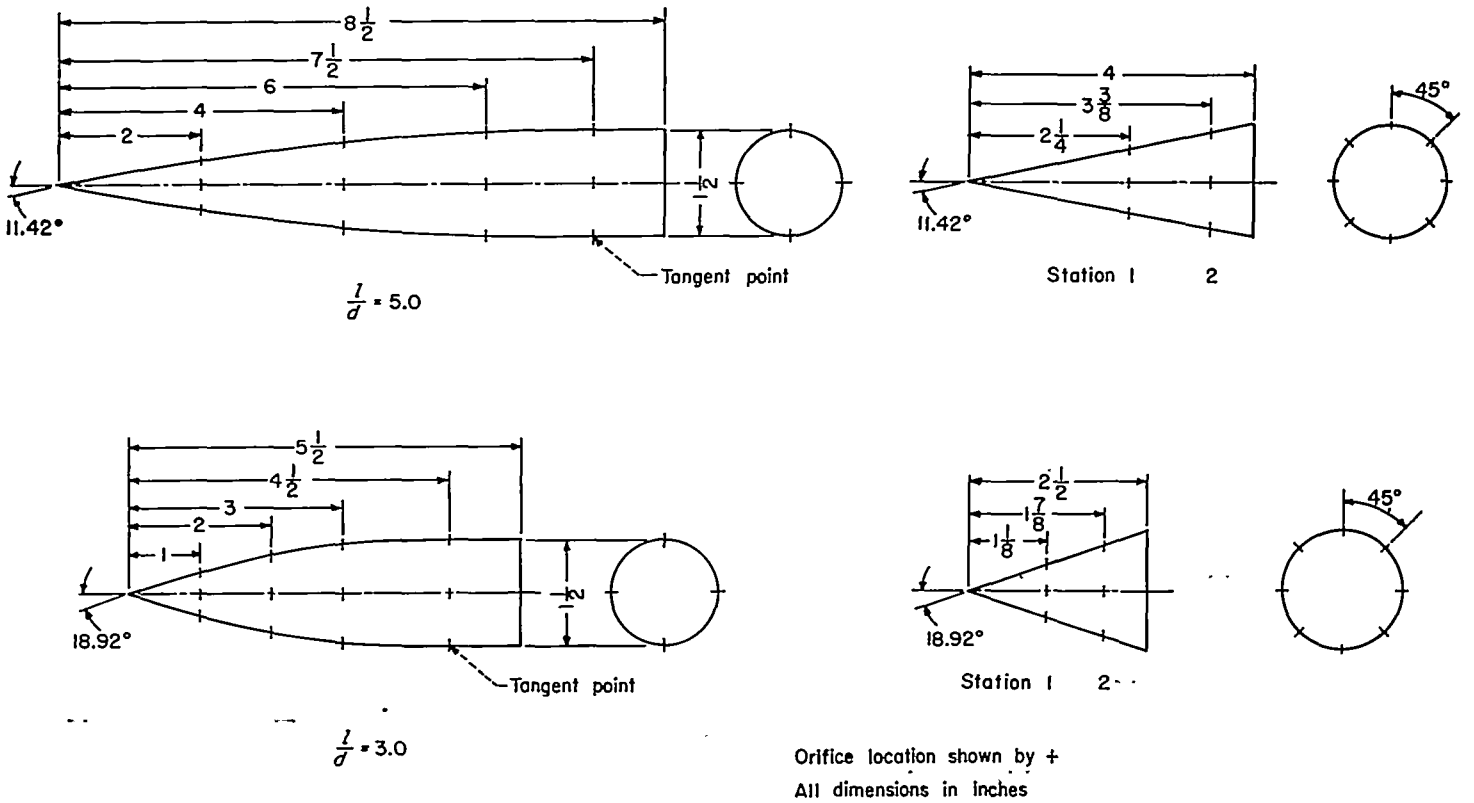

FIGURE 7.—Dimensions of pressure distribution test models showing location of pressure orifices.

TESTS AND PROCEDURE

Pressures on the model surfaces were measured at 0°, 5°, 10°, and 15° angles of attack and at test Mach numbers of 3.00, 4.25, and 5.05. Pressures on the fineness-ratio-3 ogive (as well as on the corresponding cone) were also obtained at a test Mach number of 6.30 and at 0° and 5° angles of attack. The Reynolds numbers (based on maximum diameter of the ogives) were 1.09 million at Mach numbers 3.00 and 4.25, 0.52 million at Mach number 5.05, and 0.22 million at Mach number 6.30.

The pressures around the cone surface (0° to 360°) at meridian stations 45° apart were recorded simultaneously at each Mach number and angle of attack. In the case of the two ogival models, the pressures were recorded at meridian stations 90° apart. Each model was then rotated 45° about its longitudinal axis (except at 0° angle of attack) and the process repeated.

ACCURACY OF TEST RESULTS

In the region of the test section where the models were located, the variation in Mach number did not exceed ±0.02 at Mach numbers from 3.00 to 5.05 and ±0.04 at Mach number 6.30.

The precision of the computed pressure coefficients was affected by inaccuracies in the pressure measurements, as well as uncertainties in the stream angle and the free-stream dynamic pressure. The resulting errors in the pressure coefficients were generally less than ±0.005 throughout the Mach number range for all angles of attack.

COMPARISON OF THEORY WITH EXPERIMENT AND DISCUSSION OF RESULTS

According to inviscid theory, the hypersonic similarity parameter, K, is a significant index to when the generalized shock-expansion method can be used to calculate three-dimensional flows. It was indicated in this connection that the generalized method should be applicable to bodies of revolution when K is greater than about 1. In order to check this prediction, the pressure distributions on the surfaces of two ogives (having fineness ratios 3 and 5) traveling at Mach numbers 3.00, and 4.25, and 5.05 and at angles of attack of 0°, 5°, 10°, and 15° were calculated by the methods of this paper. Pressure distributions on the fineness-ratio-3 ogive at angles of attack of 0° and 5° were also calculated for a Mach number of 6.30. The conical-flow theory presented in reference 32 was employed in these calculations for determining initial flow conditions at the vertices of both the lifting and nonlifting bodies.

Comparing first the predictions of theory with experiment [18]

[18] The experimental data shown in figure 8 and all subsequent figures represent an average of the pressures recorded at each station on a body. The scatter of data was inconsequentially small (see ref. 32).

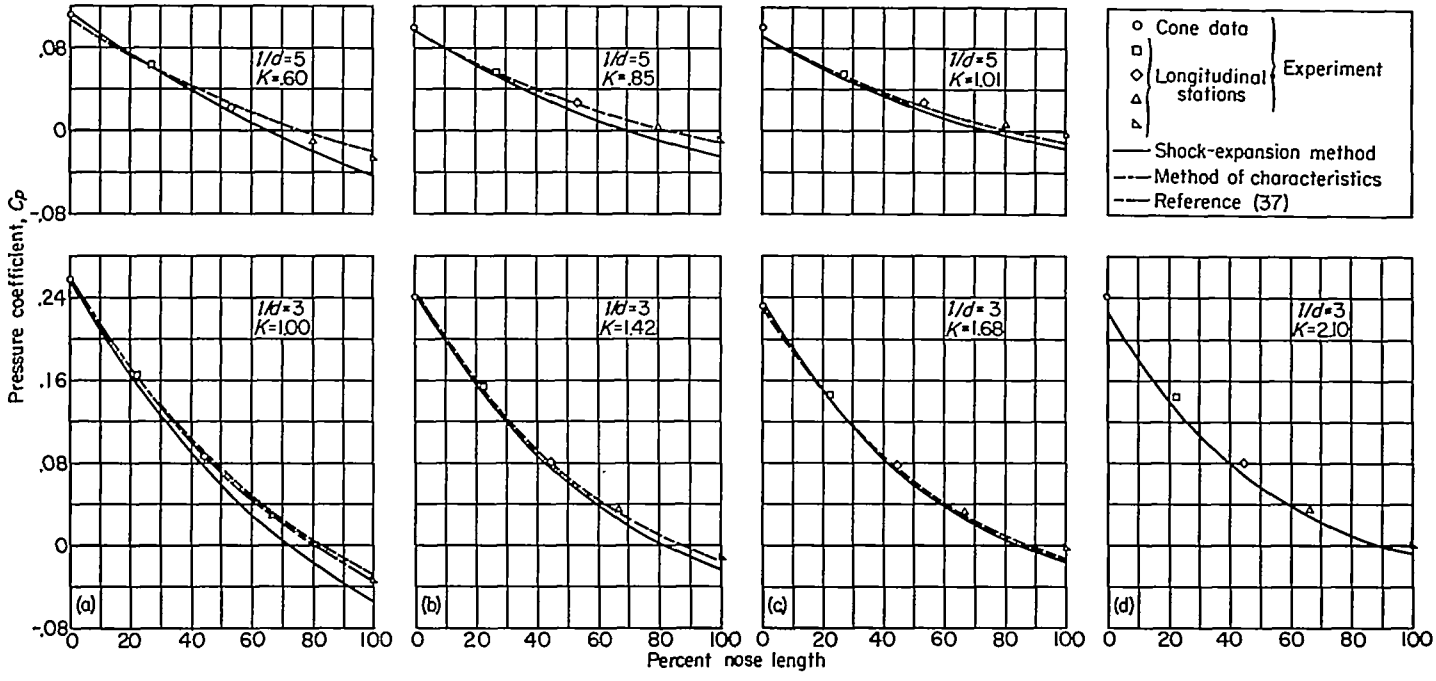

(a) $M_\infty=3.00$ (b) $M_\infty=4.25$ (c) $M_\infty=5.05$ (d) $M_\infty=6.30$

FIGURE 8.—Variation of pressure coefficient along ogives at $\alpha=0°$.

for the case of zero lift, we observe in figure 8 that the shock-expansion method predicts surface pressure coefficients close to those obtained experimentally at values of K greater than 1. As would be expected, too, the agreement between the predicted coefficients and experiment tends to improve up to a Mach number of 5.05. The results of a characteristics solution for a fineness-ratio-3 ogive at $M_\infty=3.00$ (from ref. 36) are also shown for comparative purposes. Characteristics solutions are not available for the other cases; however, the results of Rossow (obtained by correlating the pressures yielded by characteristics solutions according to the hypersonic similarity law; see ref. 37) are shown. It is evident in this figure that the agreement between these results and those yielded by the shock-expansion method improves with increasing K over the Mach number range presented. At the highest Mach number of 6.30 we observe, however; that both methods yield pressure coefficients which, although in agreement, are appreciably lower than experiment. There is no particular reason, on the basis of past experience or otherwise, to doubt the accuracy of the characteristics theory for this body. In this connection, it should be noted that the theory is generally in good agreement with experiment at all the lower Mach numbers. It seems logical, therefore, to suspect that the departure of theory from experiment at $M_\infty=6.30$ is caused by viscous effects in the flow. More specifically, it is suggested that this departure may be traced to a substantial increase in thickness of the laminar boundary layer on the ogive. The low Reynolds number of the tests and, to a somewhat lesser extent, the high Mach number could produce such an increase. This matter will be considered further in the discussion of hypersonic boundary-layer calculations presented later in the paper.

It is appropriate now to consider the reliability of the shock-expansion method for lifting bodies. As shown in figures 9, 10, and 11, the theory yields good agreement with experiment on the windward side of the fineness-ratio-5 ogive except at $M_\infty=3.00$ ($K=0.60$).[19] Disagreement is evident, however, on the leeward side of the body at all Mach numbers. In the case of the fineness-ratio-3 ogive (figs. 12, 13, and 14), agreement is generally better over the entire body at each angle of attack, particularly at the higher values of K. It will be recalled from figure 8 that at $\alpha=0°$ the longitudinal pressure distributions on both ogives indicated that the accuracy of the shock-expansion method increased as K increased. Figures 9 through 14 indicate that, as would be expected, this trend carries over to the case of lifting bodies. It is interesting to note, also, that reasonably good agreement with experiment is obtained when $K>1$ even though $\alpha\rightarrow\delta_N$. Accordingly, it is suggested that so long as $K>1$ and $\alpha/\delta_N<1$, the generalized shock-expansion method can be employed to predict surface pressures along meridian lines as though they were streamlines, with little sacrifice in accuracy. In this connection, it should be noted that the meridian lines on the extreme windward and leeward sides of the body (i. e., $\varphi=0°$ and $\varphi=180°$, respectively) are exactly streamlines.

[19] It should be noted in figure 9 that Stone's second-order solution is employed at the vertex since the conical-flow theory of reference 32 is not applicable for these conditions (i. e., $M_\infty=3.00$ and $\delta_N=11.42°$).

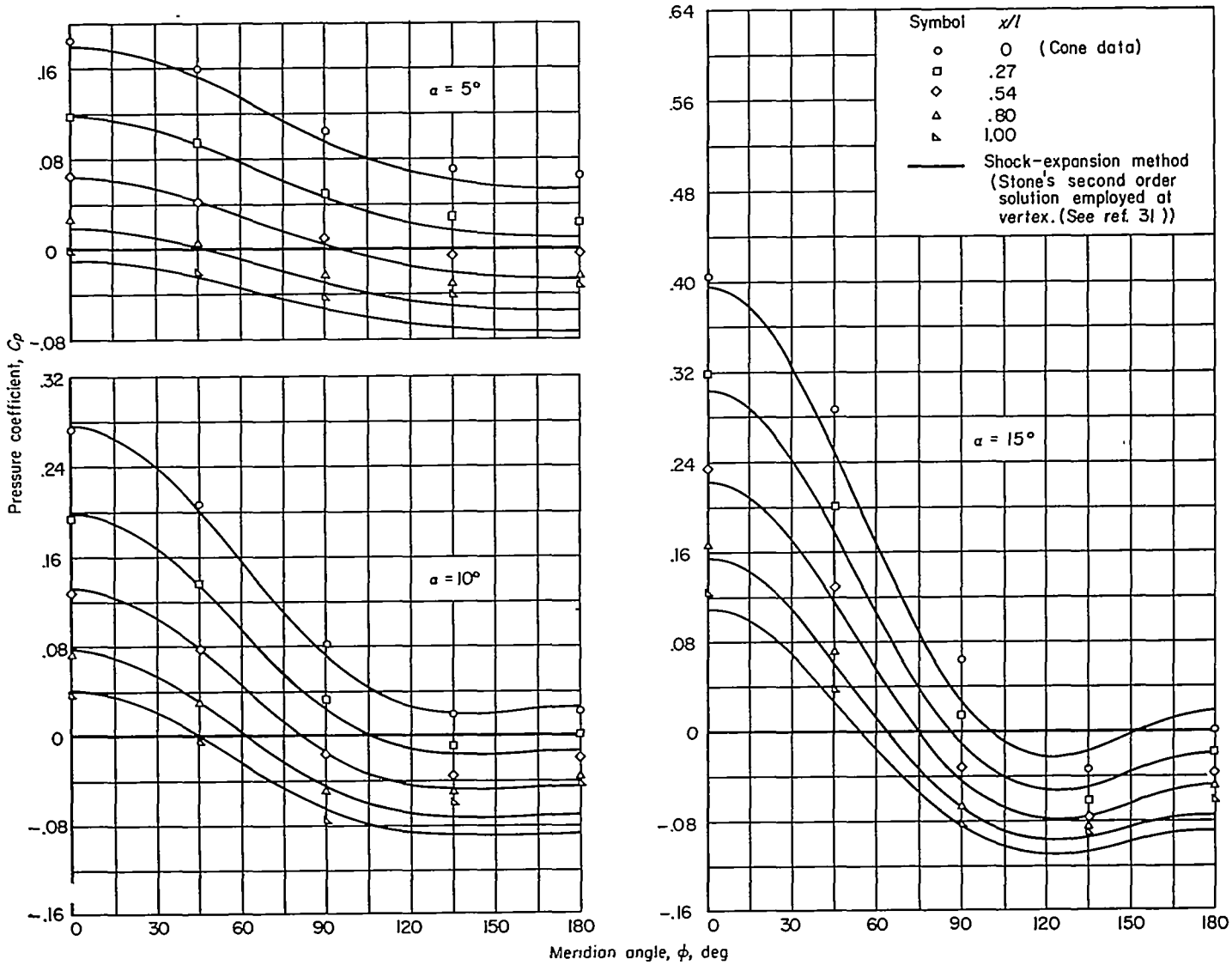

FIGURE 9.—Circumferential variation of pressure coefficient on a fineness ratio 5 ogive at $M_\infty=3.00$; $K=0.60$.

It appears in figures 9 through 14, that the most important factor influencing the accuracy of the shock-expansion method is the reliability of the conical-flow theory, since the inaccuracies at the vertex appear to be reflected strongly in the pressures downstream of the vertex. The question naturally arises, then, how good are the predictions of the method when experimentally determined initial conditions at the vertex are employed? To answer this question, the pressure coefficients on the surfaces of the two ogives under discussion were determined in the following manner. Initial conditions at the vertex were determined from the measured static pressures around a cone (corresponding to the vertex angle of the body) in conjunction with the measured shock-wave angle (in the plane $\varphi=0°$) obtained from schlieren photographs of the conical flow field. The pressure coefficients downstream of the vertex were then calculated as before. The results of these calculations for Mach numbers 3.00, 4.25, and 5.05 are compared with experiment in figures 15 and 16 for $\alpha=15°$. Results for $\alpha=15°$ are presented because at this angle of attack the applicability of the conical-flow solutions is most marginal. It is observed in figure 15 (a) that the theory yields results which indicate an underexpansion of the flow on the sides of the body ($\varphi=45°$ and $\varphi=90°$). This result is not surprising since $\alpha/\delta_N>1$ and $K<1$. It would be expected, then, that the true streamlines would deviate considerably from a meridian line. In other words, flow disturbances in planes tangent to the body at the surface are no longer small compared to those in axial planes. It can be seen from figures 15 (b) and (c) that as the Mach number, and hence, K, is increased, better agreement is obtained. This result is attributed in part to the fact that the streamlines of the flow deviate less from meridian lines as K is increased. The same general trend may be noted in figure 16 for the fineness-ratio-3 ogive. However, in this case, $\alpha/\delta_N<1$ and over-all agreement between theory and experiment is improved. In fact, good results are consistently obtained by theory except on the extreme leeward side of the body where it is probable that viscous effects are influencing the pressures. There may be some separation of flow over this portion of the body although no evidence of this could be determined from the schlieren photographs. In the case of the fineness-ratio-5 ogive, schlieren evidence

indicated flow separation on the leeward side of the body for all Mach numbers at $\alpha=15°$. It is evident from these figures that in any event the shock-expansion method will yield better results when initial conditions at the vertex are determined from cone tests rather than from presently available cone theory.

There now remains the determination of the accuracy of the predictions of the generalized shock-expansion method for the flow field (other than the surface) about a lifting body of revolution. To this end, flow in the plane of symmetry ($\varphi=0°$ and $\varphi=180°$) was calculated for each ogive traveling at a Mach number 5.05 and at an angle of attack of 10°. Flow in a side meridian plane ($\varphi=90°$) was also calculated for the fineness-ratio-3 ogive. The resulting shock-wave shapes are compared with the actual shapes (obtained from schlieren photographs) in figure 17. The theoretically determined conical shocks are also shown for contrast. In the case of the fineness-ratio-3 ogive ($K=1.68$ and $\alpha/\delta_N=0.53$), theory and experiment are observed to be in excellent agreement in the plane of symmetry. The same observations may be made for the side meridian plane. In this latter connection, it is of interest to point out that essentially the same result is obtained when the shock is assumed circular in cross-sectional planes and its location determined from the calculations in the plane of symmetry. In the case of the fineness-ratio-5 ogive, the poor agreement on the leeward side of the body is due to the limitations of the conical flow theory employed at the vertex. If experimentally determined initial conditions are employed good agreement with experiment downstream of the vertex is obtained.

Although the predictions of the generalized shock-expansion method have been checked only at the inner and outer boundaries of the flow field, it is expected that equally good results would be obtained at intermediate points in the flow field. This conclusion is based on the fact that the bow shock waves were obtained as a result of the calculations of these intermediate points.

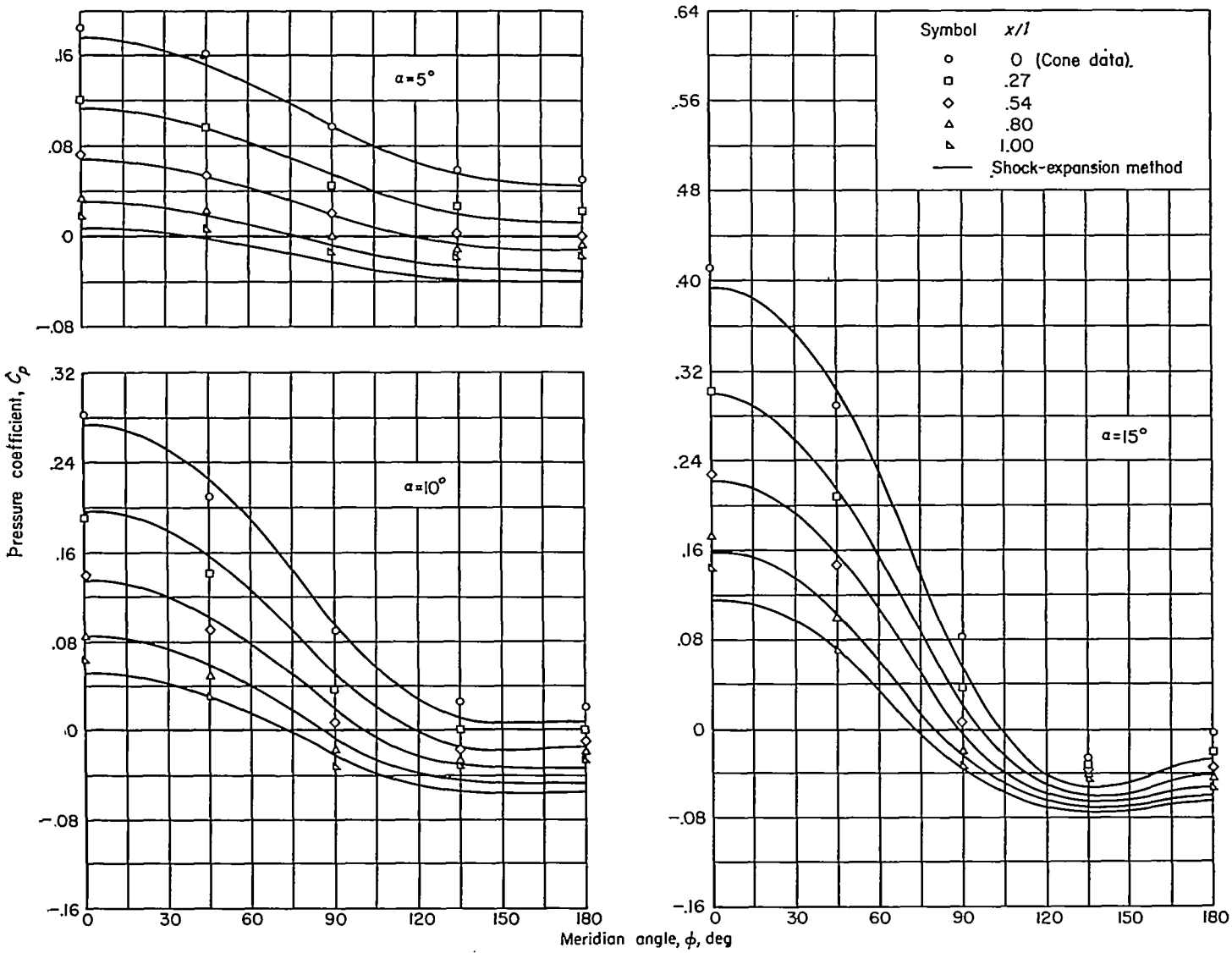

FIGURE 10.—Circumferential variation of pressure coefficient on a fineness ratio 5 ogive at $M_\infty=4.25$; $K=0.85$.

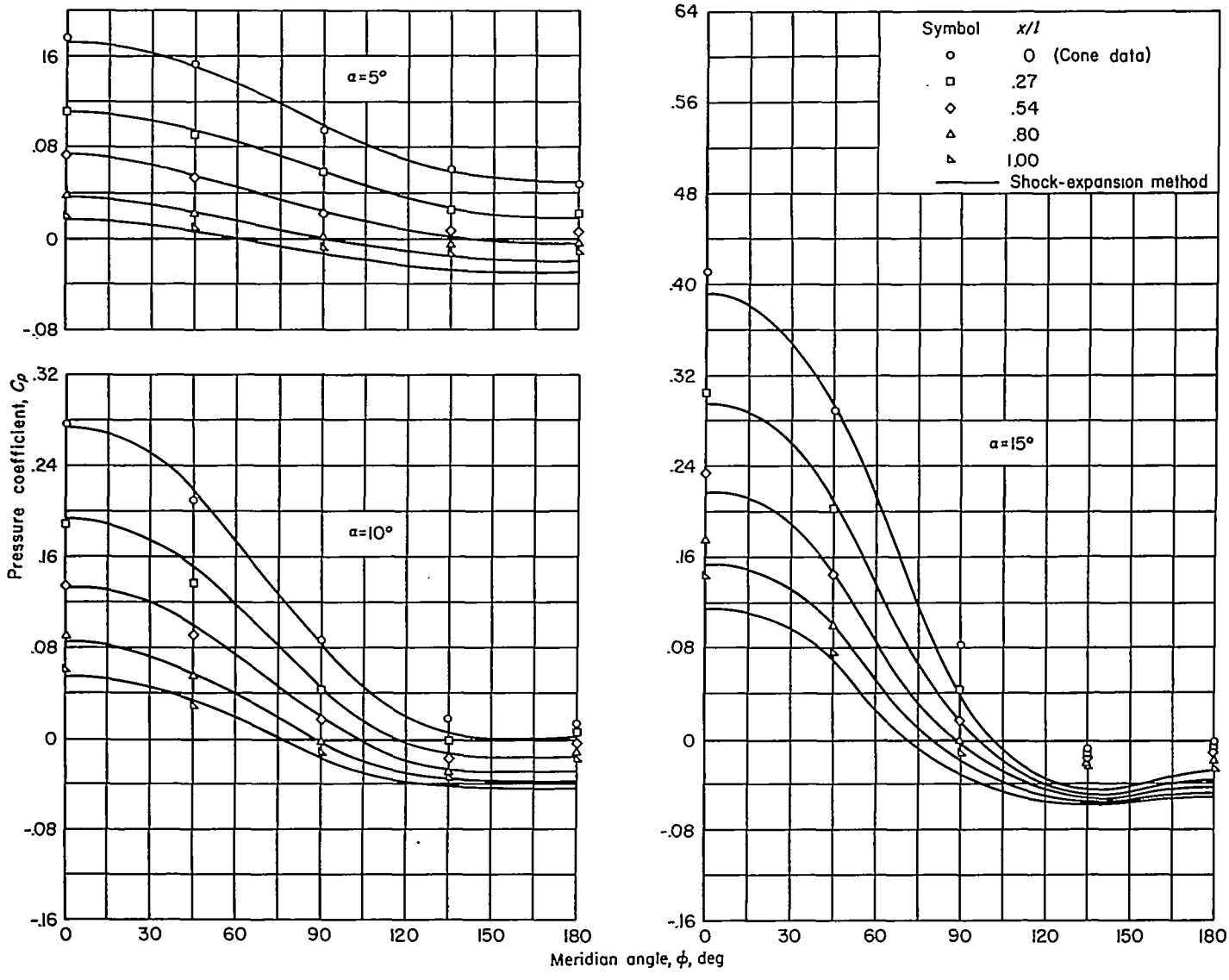

FIGURE 11.—Circumferential variation of pressure coefficient on a fineness ratio 5 ogive at $M_\infty=5.05$; $K=1.01$.

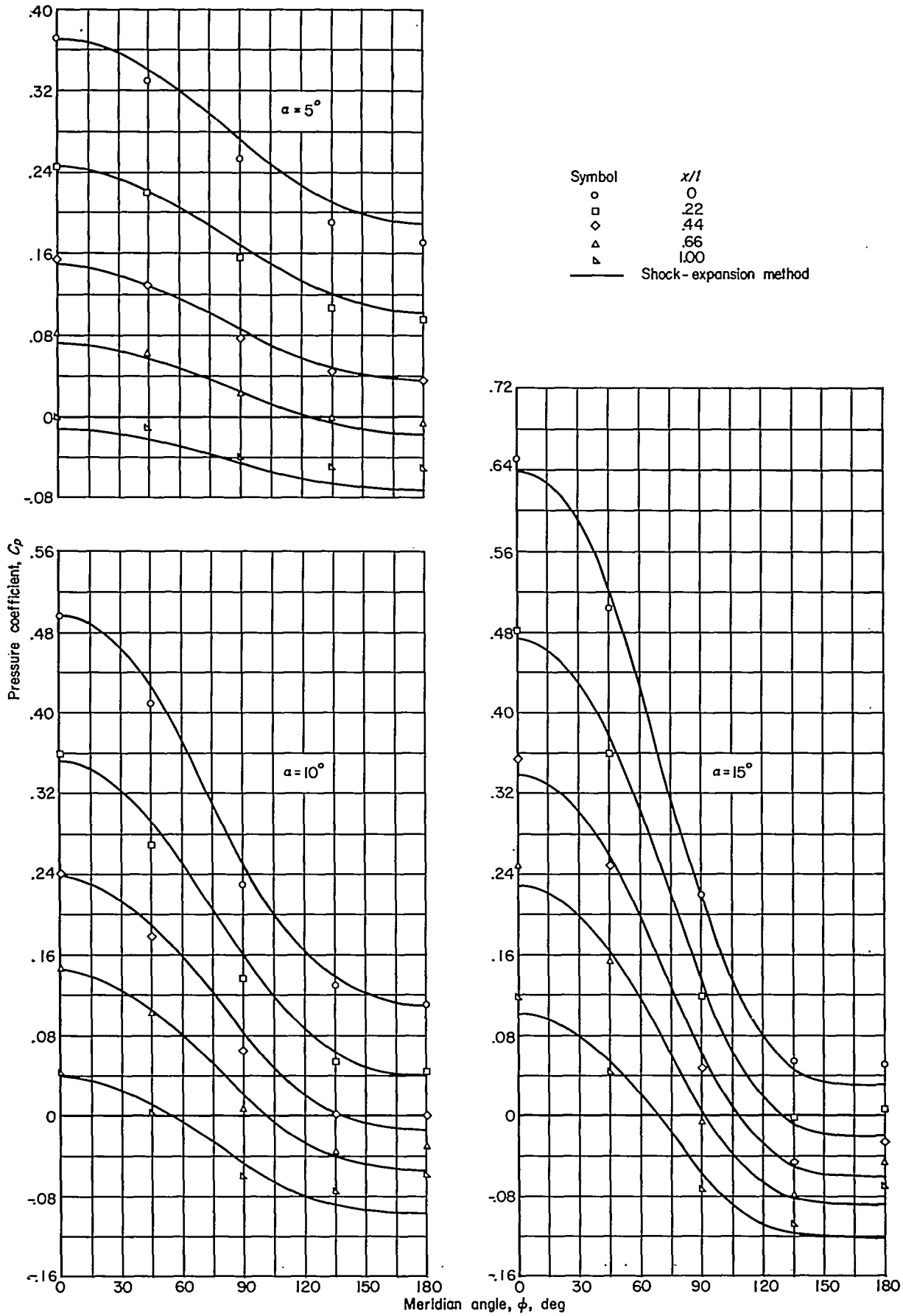

FIGURE 12.—Circumferential variation of pressure coefficient on a fineness ratio 3 ogive at $M_\infty = 3.00$; $K = 1.00$.

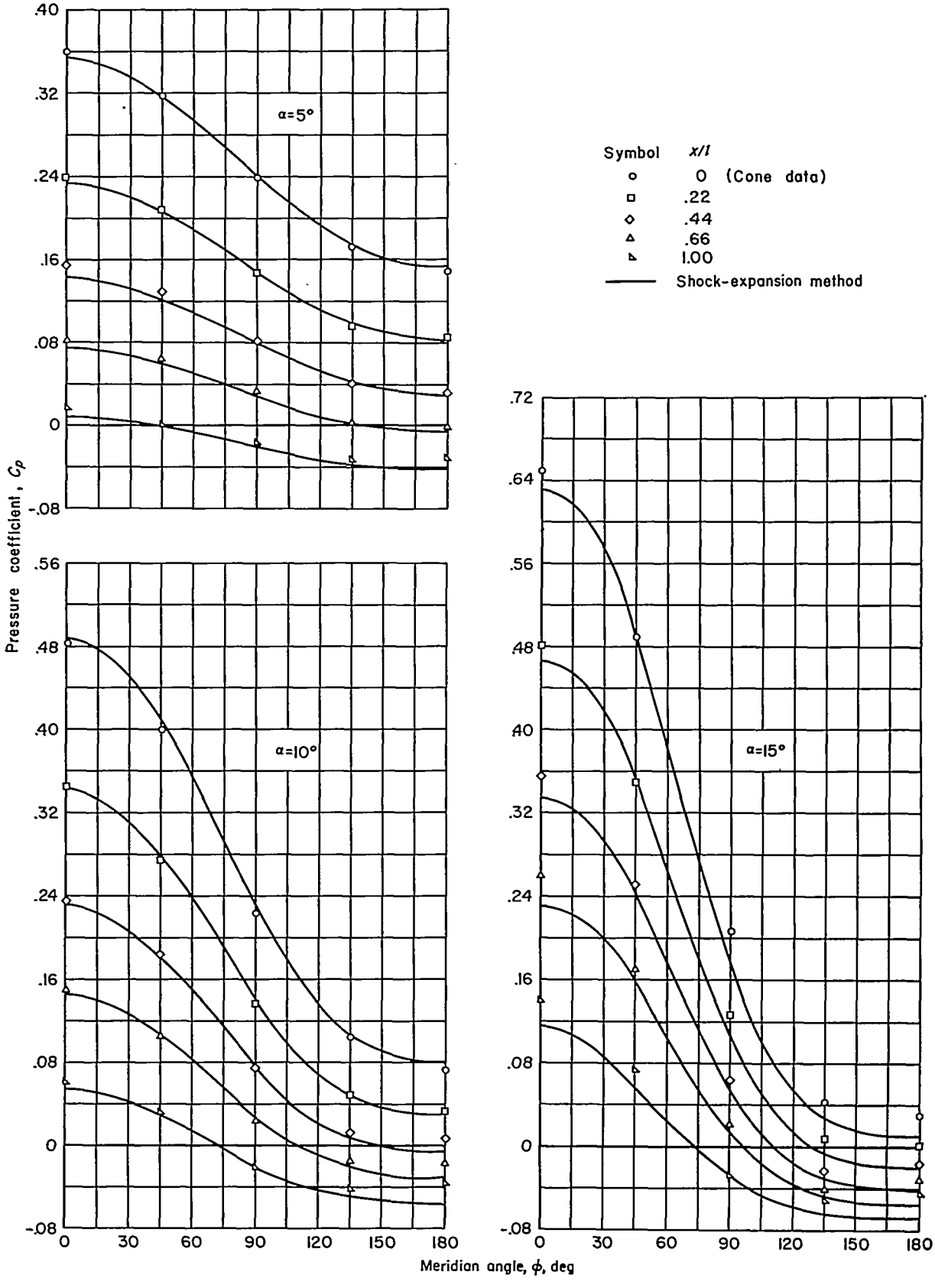

FIGURE 13.—Circumferential variation of pressure coefficient on a fineness ratio 3 ogive at $M_\infty = 4.25$; $K = 1.42$.

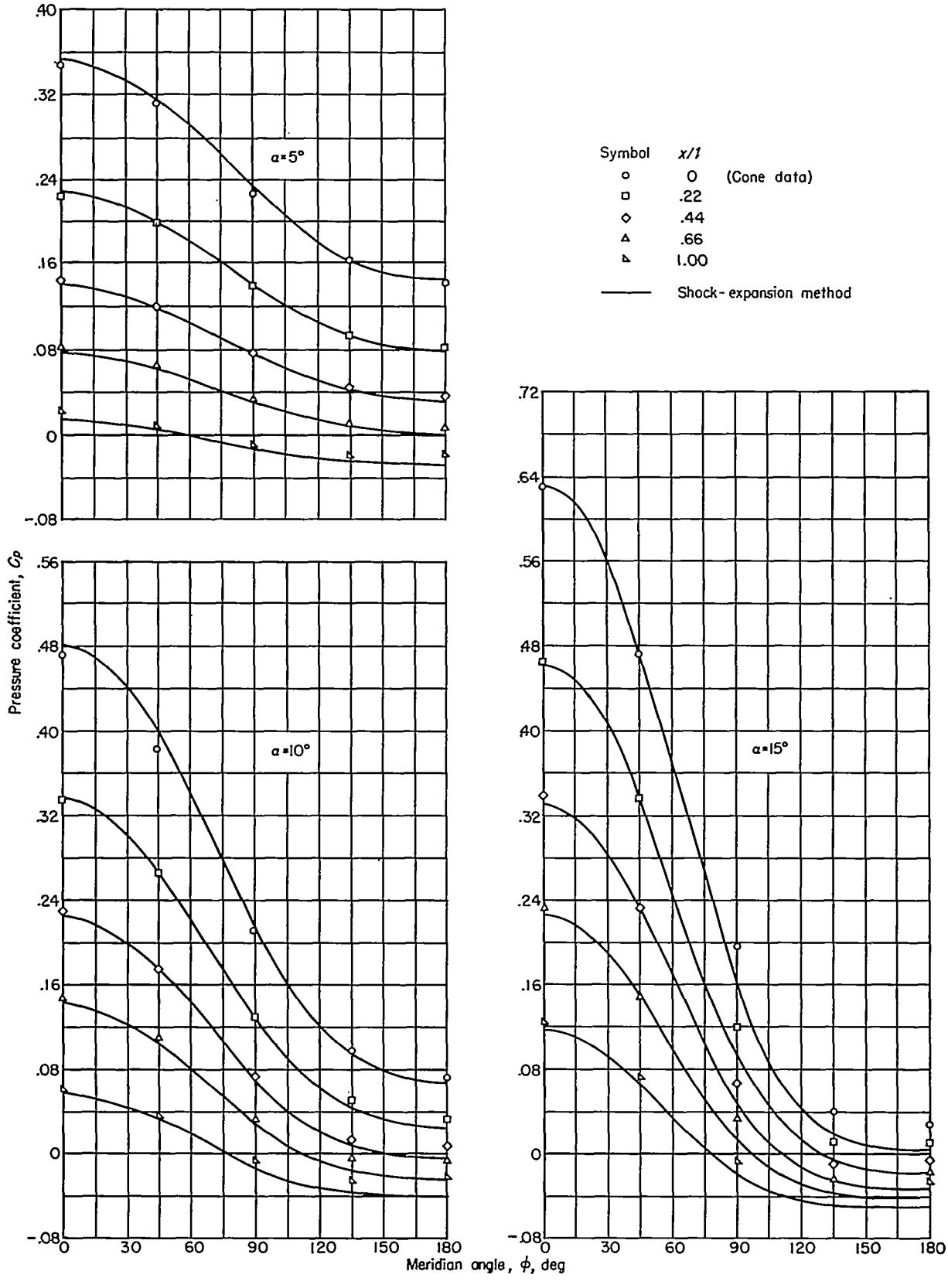

FIGURE 14.—Circumferential variation of pressure coefficient on a fineness ratio 3 ogive at $M_\infty=5.05$; $K=1.68$.

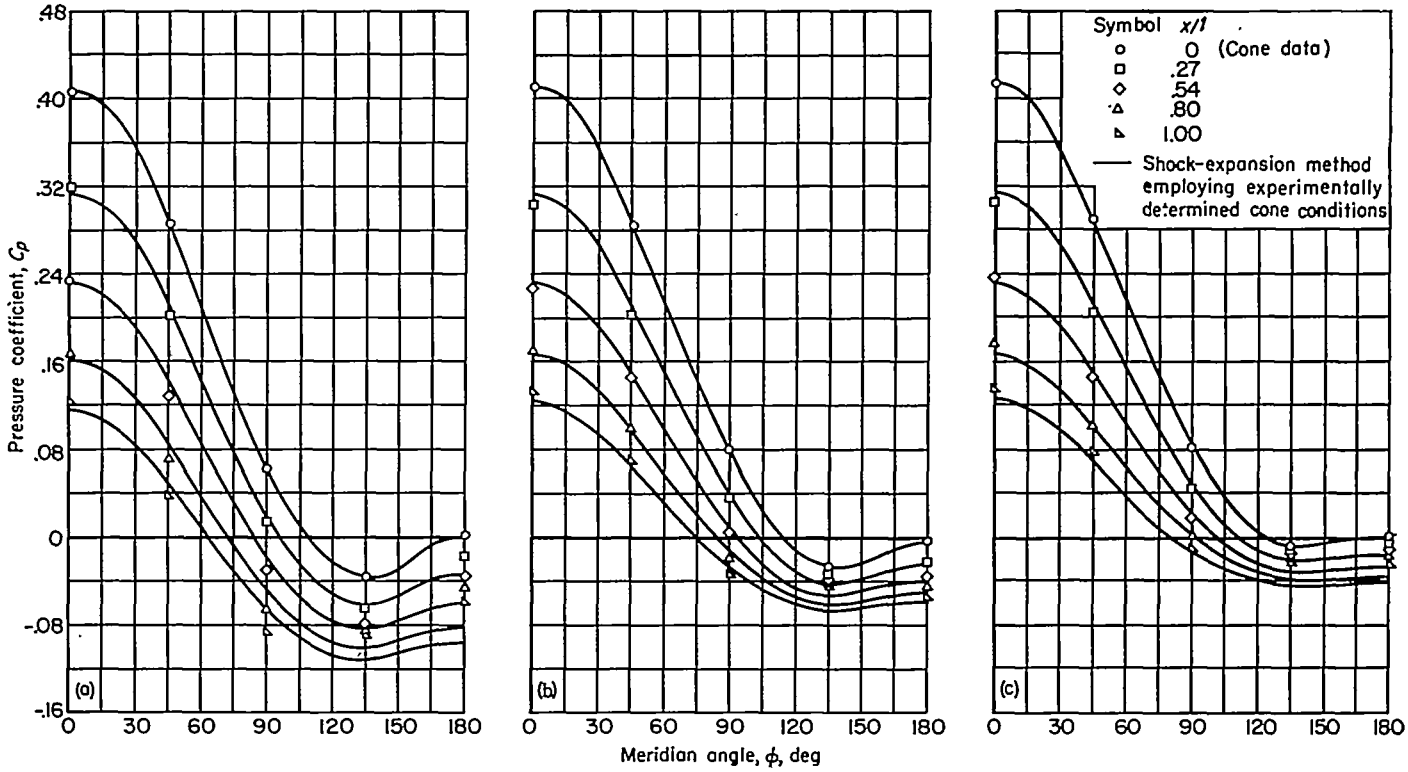

(a) $M_\infty=3.00$; $K=0.60$ (b) $M_\infty=4.25$; $K=0.85$ (c) $M_\infty=5.05$; $K=1.01$

FIGURE 15.—Circumferential variation of pressure coefficient on a fineness ratio 5 ogive at $\alpha=15°$.

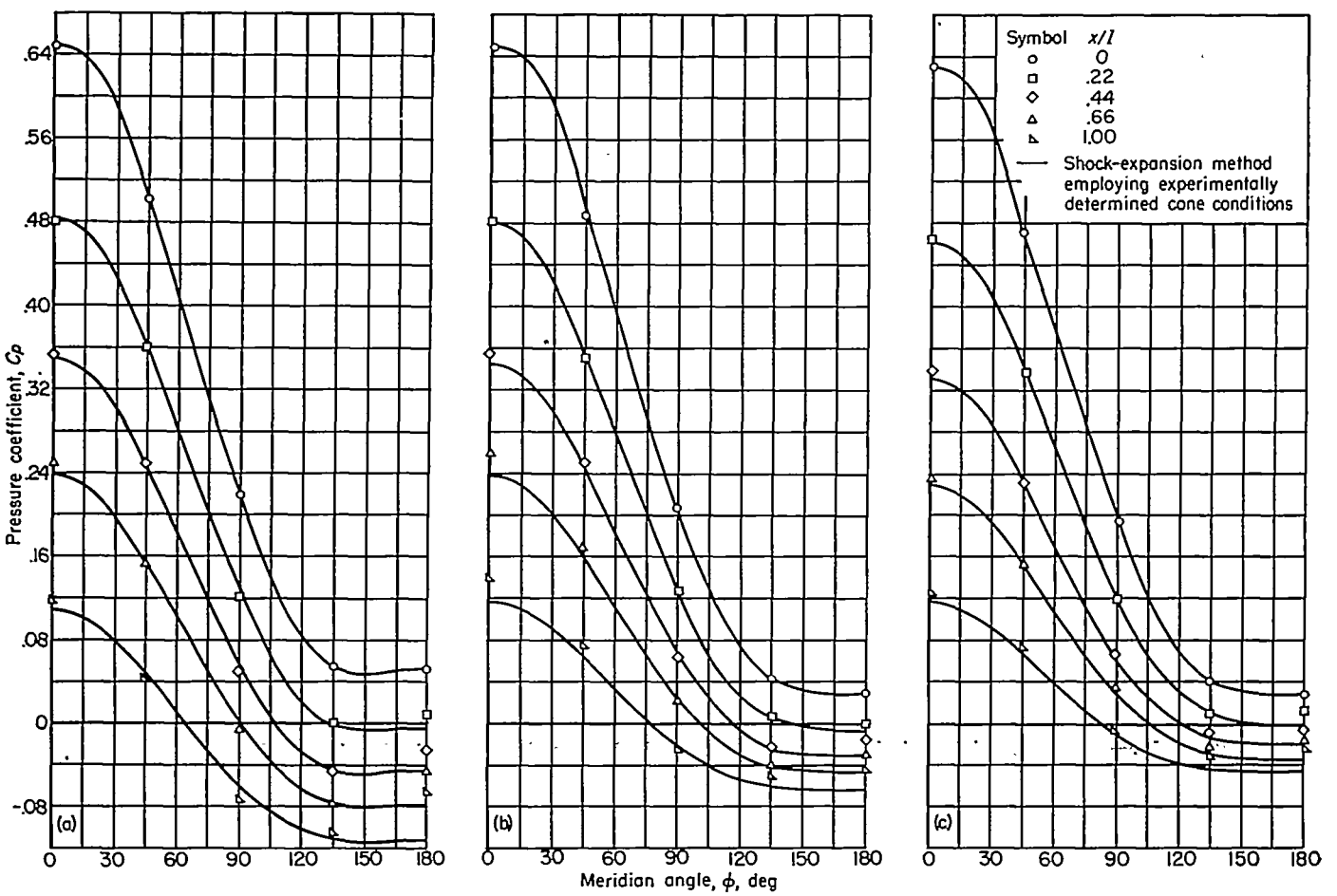

(a) $M_\infty=3.00$; $K=1.00$ (b) $M_\infty=4.25$; $K=1.42$ (c) $M_\infty=5.05$; $K=1.68$

FIGURE 16.—Circumferential variation of pressure coefficient on a fineness ratio 3 ogive at $\alpha=15°$.

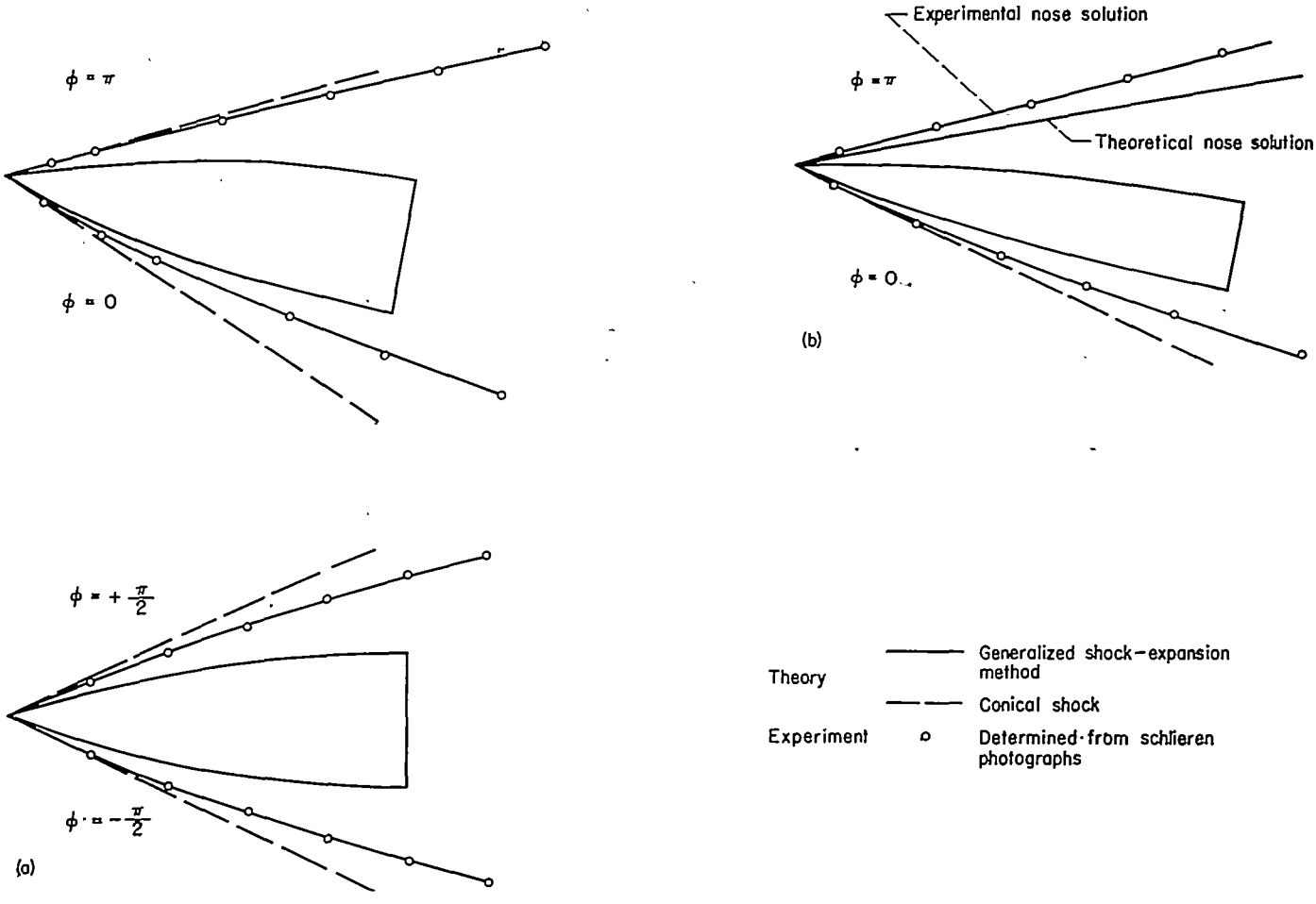

(a) $K=1.68$ (b) $K=1.01$

FIGURE 17.—Shock-wave shapes for two ogives at $M_\infty=5.05$ and $\alpha=10°$.

It is appropriate now to consider briefly the forces experienced by the ogives. To this end, normal-force coefficients were obtained by integrating the theoretical pressure distributions for the two ogives at a Mach number of 5.05. The results of these calculations are compared in figure 18 with those obtained from integrated experimental pressure distributions for values of K of 1.01 and 1.68. It is observed that although theory yields results which are, in general, higher than those obtained by experiment, agreement improves with increasing K. The same trend with K is evident for the initial normal-force-curve slopes obtained with the aid of equation (49). Axial forces were also obtained for these ogives and, as indicated in figure 18, the shock-expansion method yields generally good agreement with experiment even at a value of K as low as 1.

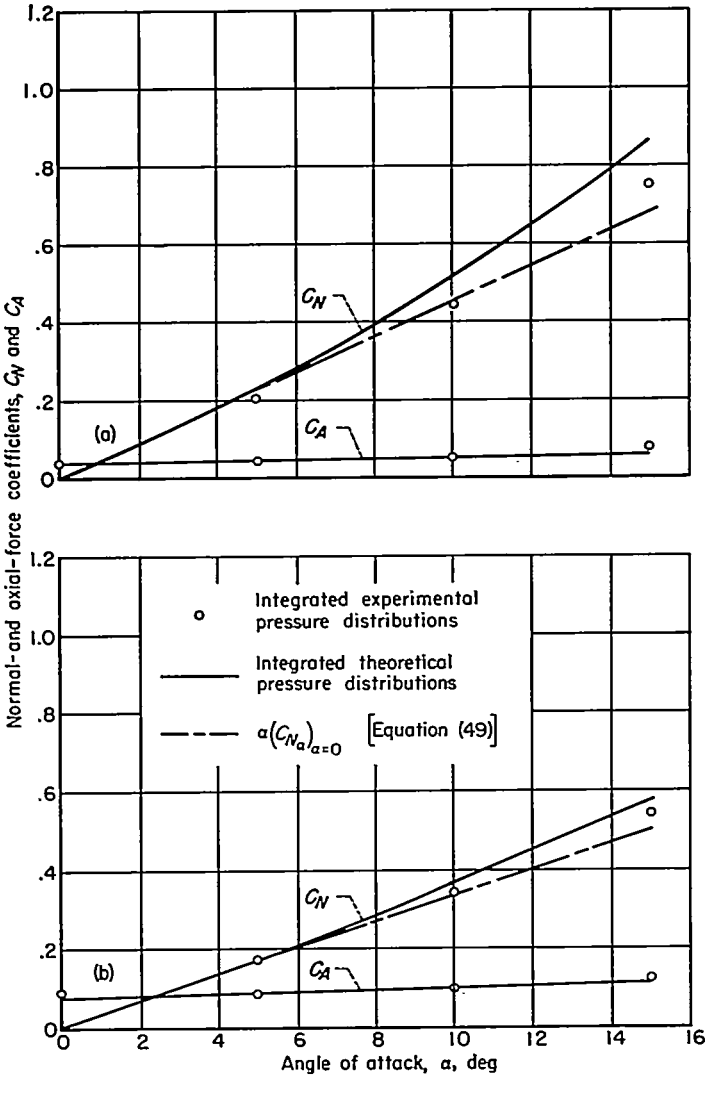

(a) $K=1.01$
(b) $K=1.68$

FIGURE 18.—Normal- and axial-force coefficients for ogives at $M_\infty=5.05$.

Let us consider now the predictions of the hypersonic slender-body theory. To this end, calculated pressure coefficients for the two ogives at $\alpha=0°$ and $\alpha=5°$ are compared with experiment in figures 19 and 20. It appears from a comparison of figures 8 and 19 that the slender-body theory will yield more accurate drag coefficients than the general theory at $\alpha=0°$, particularly at the lower values of K. This result is, of course, fortuitous. In the case of lifting bodies (fig. 20) the slender-body theory yields results which are somewhat less satisfactory at all values of K. However, the theory displays sufficient accuracy for many engineering purposes even at $K=1$. This point is particularly evident for the more slender of the two bodies as indicated in figure 20. It is also interesting to note the comparison of theory and experiment shown in figure 21 for the initial normal-force-curve slopes and centers of pressure of a family of ogives at Mach numbers from 3.00 to 6.30. The experimental data were obtained in the Ames 10- by 14-inch supersonic wind tunnel. There is good correlation of these data with $M_\infty\delta_N$, the hypersonic similarity parameter for slender bodies, and there is good agreement with theory for values of $M_\infty\delta_N$ greater than 1. In view of its simplicity, then, the hypersonic slender-body theory should prove useful and its application is further facilitated by the presentation in this paper of tabulated values of the pertinent flow parameters for selected values of $M_\infty\delta_N$ and α/δ_N (see table I).

Up to this point we have been concerned almost entirely with the inviscid theory and its comparison with experimental data relatively free of effects of viscosity. As a final point, it is appropriate to test the two-dimensional boundary-layer concept of this paper by considering flows which are significantly influenced by viscous effects.

In this connection it was noted early in the previous discussion that inviscid theory yielded pressure coefficients which were substantially lower than experiment at $M_\infty=6.30$. This discrepancy was traced to the thick laminar boundary layer on the test body. According to theory it should be possible to calculate this boundary layer approximately by means of simple two-dimensional techniques. This possibility was checked by calculating the laminar boundary layer on the fineness-ratio-3 ogive at a Mach number of 6.30 and angles of attack of 0° and 5°. The two-dimensional theory of reference 38 was employed.[20] The body ordinates were increased by an amount equal to the displacement thickness of the boundary layer. The pressure distribution about the distorted body was then obtained with the generalized shock-expansion method. These corrected pressure distributions and the original uncorrected distributions are presented in figure 22 along with experiment. It is observed that while uncorrected pressures are definitely low, the corrected pressure distributions are in good agreement with experiment. In this case, then, relatively simple two-dimensional methods of correcting pressure distributions for the presence of the boundary layer are, as indicated by theory, applicable to the body of revolution.

[20] The theory breaks down at the vertex of the body, much as at the leading edge of an airfoil. It is therefore not applied in this region, and, consistent with a practice successfully employed with airfoils, viscous effects are ignored in calculating flow at the vertex.

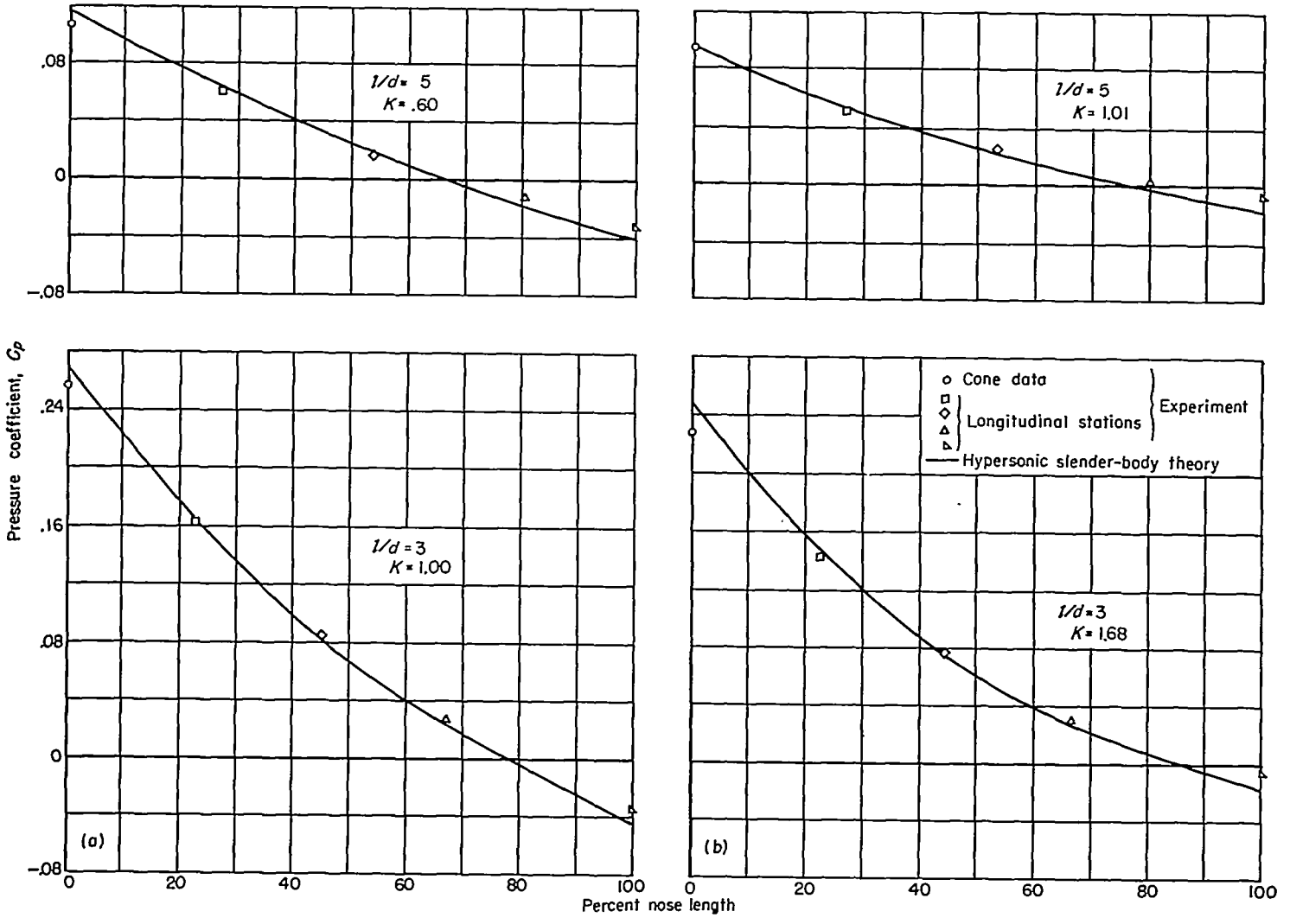

(a) $M_\infty = 3.00$ (b) $M_\infty = 5.05$

FIGURE 19.—Pressure distributions predicted by hypersonic slender-body theory for ogives at $\alpha = 0°$.

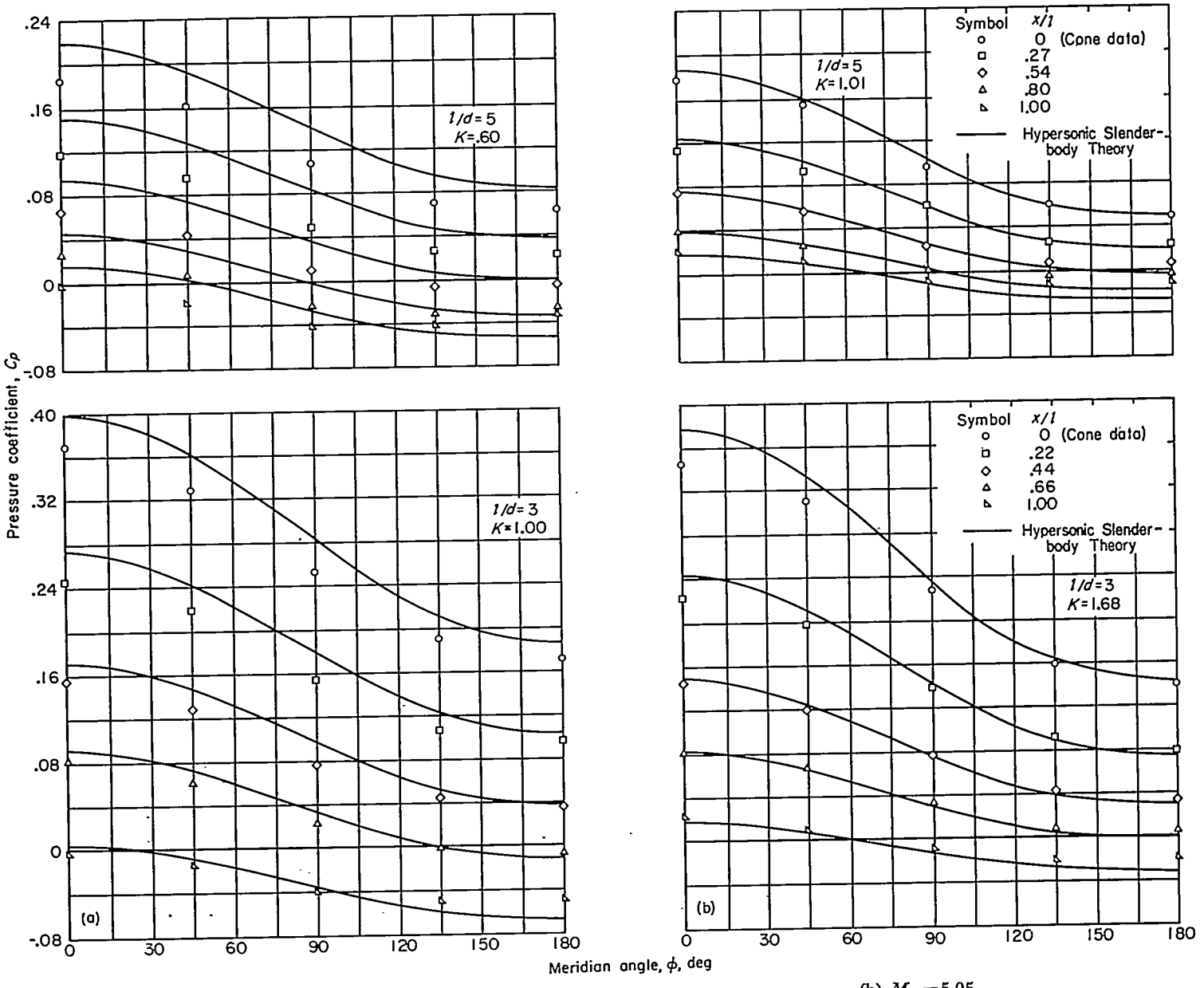

(a) $M_\infty = 3.00$ (b) $M_\infty = 5.05$

FIGURE 20.—Pressure distributions predicted by hypersonic slender-body theory for ogives at $\alpha = 5°$.

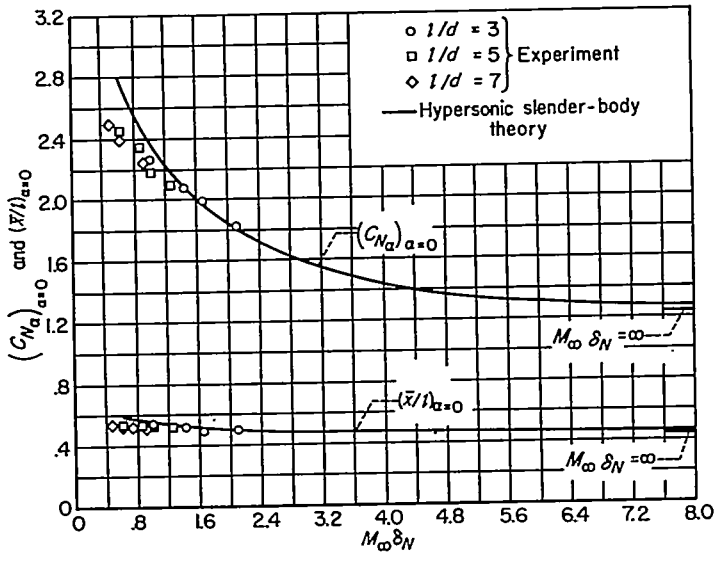

FIGURE 21.—Normal-force derivatives and centers of pressure for ogives ($\alpha \to 0$).

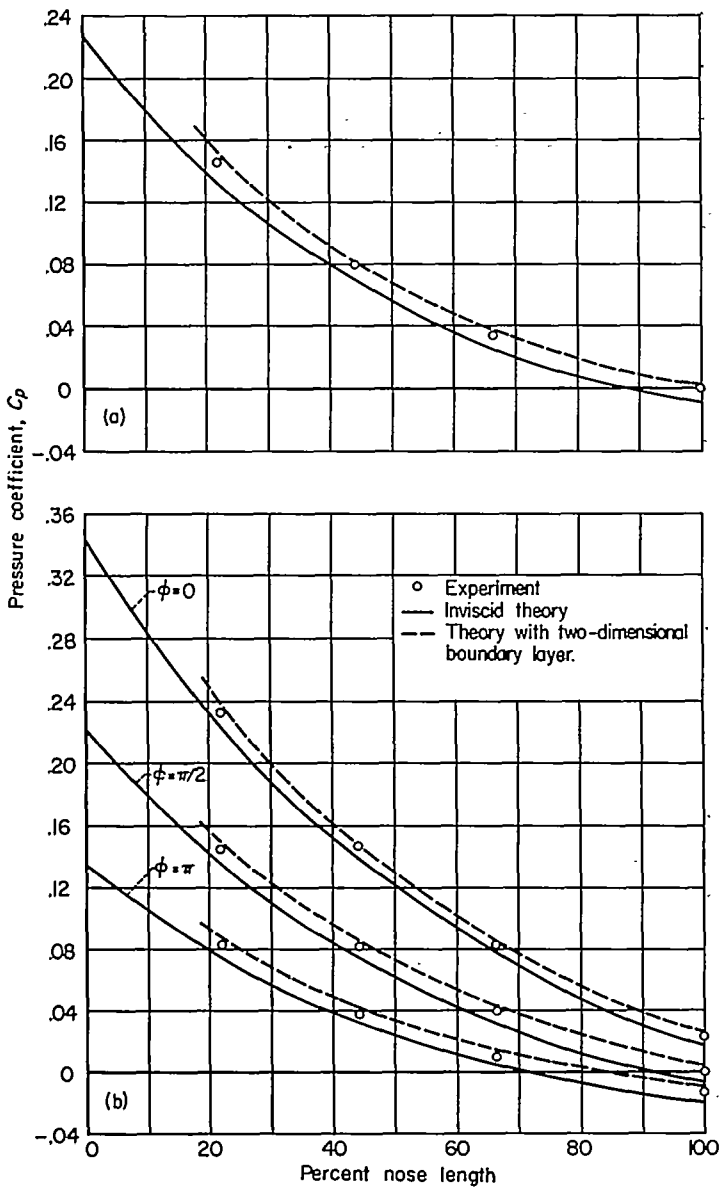

(a) $\alpha=0°$
(b) $\alpha=5°$

FIGURE 22.—Effect of boundary layer on pressures acting on a fineness ratio 3 ogive at $M_\infty=6.30$.

CONCLUDING REMARKS

A method of characteristics employing pressure and flow inclination angles as dependent variables was used to obtain a simplified approximate method for calculating three-dimensional flows at high supersonic speeds. It was found that when the flight Mach number is sufficiently large compared to 1, flow in the osculating planes of streamlines in regions free of shock waves may be of the generalized Prandtl-Meyer type—surface streamlines in this event may be treated as geodesics. In the case of slender bodies, these results apply to nonsteady as well as steady flows. The two-dimensional approach to three-dimensional hypersonic flows was also extended to steady boundary-layer flows.

Bodies of revolution in steady hypersonic flight were considered as an example of shapes producing three-dimensional flow fields which appear locally two-dimensional. With the assumption of conical flow at the vertex and small angles of attack, simple approximate solutions were obtained which yield the Mach number and pressure distributions on the surfaces of such bodies. Surface streamlines were approximated by meridian lines and the flow field in meridian planes was calculated by means of a generalized shock-expansion method. In the special case of slender bodies, simple explicit expressions were obtained for the Mach number and pressure distribution on the surface.

Surface pressures and shock-wave shapes were obtained experimentally at Mach numbers from 3.00 to 5.05 for two ogives having fineness ratios 3 and 5 and for two cones having the same vertex angles as the ogives. The predictions of the methods of this paper for the surface pressures and shock-wave shapes were found to be in good agreement with experiment at values of K of about 1, or greater, when α/δ_N (the ratio of angle of attack to semivertex angle) was about 1/2 or less. For increasing values of this parameter, agreement deteriorated but was still reasonably good for values of α/δ_N up to about 1. Experimental surface pressures at a Mach number of 6.30 and angles of attack of 0° and 5° were also obtained for the fineness-ratio-3 ogive. The predictions of the shock-expansion method when employed in conjunction with a two-dimensional boundary-layer calculation were found to be in good agreement with experiment.

In view of these results, it is concluded that the generalized shock-expansion method should prove useful in treating three-dimensional hypersonic flow fields about practical aerodynamic configurations. Furthermore, it is indicated that methods of treating two-dimensional hypersonic boundary layers may, in like manner, prove useful in predicting three-dimensional hypersonic boundary layers.

AMES AERONAUTICAL LABORATORY
NATIONAL ADVISORY COMMITTEE FOR AERONAUTICS
MOFFETT FIELD, CALIF., *Aug. 15, 1952*

REFERENCES

1. Tsien, Hsue-Shen: Similarity Laws of Hypersonic Flows. Jour. Math. and Phys., vol. 25, no. 3, Oct. 1946, pp. 247–251.
2. Hayes, Wallace D.: On Hypersonic Similitude. Quart. Appl. Math., vol. V, no. 1, Apr. 1947, pp. 105–106.
3. Hamaker, Frank M., Neice, Stanford E., and Eggers, A. J., Jr.: The Similarity Law for Hypersonic Flow About Slender Three-Dimensional Shapes. NACA TN 2443, 1951.
4. Lin, C. C., Reissner, E., and Tsien, H. S.: On Two-Dimensional Nonsteady Motion of a Slender Body in a Compressible Fluid. Jour. Math. and Phys., vol. 27, no. 3, Oct. 1948, pp. 220–231.
5. Hamaker, Frank M., and Wong, Thomas J.: The Similarity Law for Nonsteady Hypersonic Flows and Requirements for the Dynamical Similarity of Related Bodies in Free Flight. NACA TN 2631, 1952.
6. Guderley, G.: Extension of the Characteristics Method. British R. A. E. Library Translation No. 151. (From Lilienthal-Gesellschaft Rep. 139, pt. 2, pp. 15–22), Jan. 1947.
7. Eggers, A. J., Jr., Syvertson, Clarence A., and Kraus, Samuel: A Study of Inviscid Flow About Airfoils at High Supersonic Speeds. NACA Rep. 1123, 1953. (Formerly NACA TN 2646)
8. Mass. Inst. Tech., Dept. Elec. Engr., Center of Analysis: Tables of Supersonic Flow Around Cones. By the staff of the Computing Section, Center of Analysis, under the direction of Zdenek Kopal. Cambridge, 1947. Tech. Rep. No. 1.
9. Van Dyke, Milton D.: A Study of Second-Order Supersonic-Flow Theory. NACA TN 2200, 1951.
10. Eggers, A. J., Jr., and Savin, Raymond C.: Approximate Methods for Calculating the Flow About Nonlifting Bodies of Revolution at High Supersonic Airspeeds. NACA TN 2579, 1951.
11. Stone, A. H.: On Supersonic Flow Past a Slightly Yawing Cone. Jour. Math. and Phys., vol. XXVII, no. 1, Apr. 1948, pp. 67–81.
12. Mass. Inst. Tech., Dept. Elec. Engr., Center of Analysis: Tables of Supersonic Flow Around Yawing Cones. By the staff of the Computing Section, Center of Analysis, under the direction of Zdenek Kopal. Cambridge, 1947. Tech. Rep. No. 3.
13. Ferri, Antonio: Supersonic Flow Around Circular Cones at Angles of Attack. NACA Rep. 1045, 1951. (Formerly NACA TN 2236)
14. Ferri, Antonio: The Method of Characteristics for the Determination of Supersonic Flow Over Bodies of Revolution at Small Angles of Attack. NACA Rep. 1044, 1951. (Formerly NACA TN 1809)
15. Moeckl, W. E.: Use of Characteristic Surfaces for Unsymmetrical Supersonic Flow Problems. NACA TN 1849, 1949.
16. Coburn, N., and Dolph, C. L.: The Method of Characteristics in Three-Dimensional Stationary Supersonic Flow of a Compressible Gas. Proc. Symp. Appl. Math., vol. I, pp. 55–66. Amer. Math. Soc., New York, 1949.
17. Thornhill, C. K.: The Numerical Method of Characteristics for Hyperbolic Problems in Three Independent Variables. Armament Research Establishment. Rep. 29/48, British Ministry of Supply, Sept. 1948.
18. Sauer, Robert: Recent Advances in the Theory of Supersonic Flow. NAVORD Rep. 1593, Mar. 20, 1951.
19. Coburn, N.: Characteristic Directions in Three-Dimensional Supersonic Flows. Amer. Math. Soc. Proc., I, 1950, pp. 241–245.
20. Eggers, A. J., Jr.: On the Calculation of Flow About Objects Traveling at High Supersonic Speeds. NACA TN 2811, 1952.
21. Busemann, A., and Walchner, O.: Airfoil Characteristics at Supersonic Velocities. British R. T. P. Trans. 1786. (Forschung auf dem Gebiete des Ingenieurwesens, vol. 4, no. 2, March/April 1933, pp. 87–92.)
22. Moore, Franklin K.: Second Approximation to Supersonic Conical Flows. Jour. Aero. Sci., vol. 17, no. 6, June 1950, pp. 328–334, 383.
23. Newton, Isaac: Principia—Motte's Translation Revised. Univ. of Calif. Press, 1946.
24. Busemann, A.: Flüssigkeits-und Gasbewegung. Handwörterbuch der Naturwissenschaften, Zweite Auflage, Gustav Fischer, Jena, 1933, pp. 266–279.
25. Ivey, H. Reese, Klunker, E. Bernard, and Bowen, Edward N.: A Method for Determining the Aerodynamic Characteristics of Two- and Three-Dimensional Shapes at Hypersonic Speeds. NACA TN 1613, 1948.
26. Grimminger, G., Williams, E. P., and Young, G. B. W.: Lift on Inclined Bodies of Revolution in Hypersonic Flow. Jour. Aero. Sci., vol. 17, no. 11, Nov. 1950, pp. 675–690.
27. Oswatitsch, Klaus: Similarity Laws for Hypersonic Flows. Kungl. Tekniska Högskolan, Stockholm, Institutionen för Ftygteknik, Tech. Note 16, July 19, 1950, pp. 4–5.
28. Graustein, William C.: Differential Geometry. MacMillan Co., 1935, pp. 149–156.
29. Lighthill, M. J.: Oscillating Airfoils at High Mach Number. Jour. Aero. Sci., vol. 20, no. 6, June 1953, pp. 402–406.
30. Mangler, W.: Compressible Boundary Layers on Bodies of Revolution. Ministry of Aircraft Production, Volkenrode, Rep. and Trans. No. 47, Mar. 15, 1946.
31. Roberts, Richard C., and Riley, James D.: A Guide to the Use of the M. I. T. Cone Tables. NAVORD Rep. 2606 (Aero Ballistic Research Rep. 123), Apr. 1, 1953.
32. Savin, Raymond C.: Application of the Generalized Shock-Expansion Method to Inclined Bodies of Revolution Traveling at High Supersonic Airspeeds. NACA TN 3349, 1955.
33. Staff of the Ames Aeronautical Laboratory: Equations, Tables, and Charts for Compressible Flow. NACA Rep. 1135, 1953.
34. Eggers, A. J., Jr., and Kraus, Samuel: Approximate Calculation of Axisymmetric Flow Near the Vertex of a Body Traveling at High Supersonic Speeds. Jour. Aero. Sci., vol. 20, no. 3, Mar. 1953, pp. 215–217.
35. Eggers, A. J., Jr., and Nothwang, George J.: The Ames 10- by 14-Inch Supersonic Wind Tunnel. NACA TN 3095, 1954.
36. Ehret, Dorris M.: Accuracy of Approximate Methods for Predicting Pressures on Pointed Nonlifting Bodies of Revolution in Supersonic Flow. NACA TN 2764, 1952.
37. Rossow, Vernon J.: Applicability of the Hypersonic Similarity Rule to Pressure Distributions which Include the Effects of Rotation for Bodies of Revolution at Zero Angle of Attack. NACA TN 2399, 1951.
38. Bertram, Mitchel H.: An Approximate Method for Determining the Displacement Effects and Viscous Drag of Laminar boundary Layers in Two-Dimensional Hypersonic Flow. NACA TN 2773, 1952.

TABLE I.—TABLE OF FUNCTIONS FOR HYPERSONIC SLENDER-BODY METHOD

$\frac{p_s/p_\infty}{(M_\infty \delta_N)^2}$ for $\varphi=0°$

$M_\infty\delta_N$ \ α/δ_N	0	0.20	0.40	0.60	0.80	1.00
0.60	4.178	4.753	5.406	6.143	6.969	7.817
.80	2.963	3.517	4.161	4.898	5.732	6.665
1.00	2.400	2.952	3.599	4.343	5.188	6.131
1.20	2.094	2.649	3.301	4.052	4.903	5.853
1.40	1.910	2.468	3.125	3.881	4.737	5.691
1.60	1.791	2.352	3.013	3.773	4.633	5.589
1.80	1.709	2.273	2.937	3.700	4.562	5.518
2.00	1.650	2.217	2.884	3.648	4.512	5.471
2.50	1.560	2.132	2.802	3.569	4.436	5.398
3.00	1.511	2.086	2.759	3.529	4.396	5.359
4.00	1.462	2.041	2.716	3.489	4.357	5.321
6.00	1.428	2.008	2.686	3.459	4.329	5.294
10.00	1.410	1.992	2.671	3.446	4.315	5.280
∞	1.400	1.983	2.662	3.437	4.307	5.272

$\frac{(M_s)_{\varphi=0}}{M_N}$ for $\varphi=30°$

$M_\infty\delta_N$ \ α/δ_N	0	0.20	0.40	0.60	0.80	1.00
0.60	1.021	1.021	1.020	1.019	1.017	1.014
.80	1.021	1.019	1.017	1.014	1.012	1.009
1.00	1.019	1.017	1.013	1.010	1.007	1.004
1.20	1.017	1.014	1.010	1.006	1.003	.9996
1.40	1.016	1.012	1.007	1.004	.9998	.9964
1.60	1.014	1.010	1.005	1.001	.9974	.9939
1.80	1.013	1.008	1.004	.9994	.9955	.9919
2.00	1.012	1.007	1.002	.9981	.9940	.9903
2.50	1.011	1.005	1.000	.9964	.9914	.9876
3.00	1.010	1.004	.9988	.9940	.9897	.9857
4.00	1.009	1.003	.9972	.9924	.9878	.9838
6.00	1.008	1.002	.9960	.9910	.9863	.9822
10.00	1.007	1.001	.9954	.9903	.9856	.9812
∞	1.007	1.001	.9950	.9899	.9851	.9808

$\frac{(M_s)_{\varphi=0}}{M_N}$ for $\varphi=120°$

$M_\infty\delta_N$ \ α/δ_N	0	0.20	0.40	0.60	0.80	1.00
0.60	1.021	1.002	0.9803	0.9556	0.9271	0.8942
.80	1.021	.9918	.9600	.9247	.8850	.8396
1.00	1.019	.9812	.9405	.8961	.8466	.7891
1.20	1.017	.9717	.9238	.8720	.8139	.7460
1.40	1.016	.9638	.9102	.8527	.7876	.7109
1.60	1.014	.9574	.8993	.8371	.7666	.6828
1.80	1.013	.9523	.8907	.8247	.7501	.6607
2.00	1.012	.9483	.8839	.8152	.7372	.6436
2.50	1.011	.9412	.8723	.7989	.7164	.6161
3.00	1.010	.9369	.8656	.7903	.7053	.6024
4.00	1.009	.9324	.8587	.7820	.6967	.5931
6.00	1.008	.9289	.8540	.7776	.6963	----
10.00	1.007	.9271	.8518	.7768	----	----
∞	1.007	.9260	.8507	---	---	----

$M_s\delta_N$ for $\varphi=0°$

$M_\infty\delta_N$ \ α/δ_N	0	0.20	0.40	0.60	0.80	1.00
.60	.5655	.5577	.5432	.5319	.5203	.5095
.80	.7274	.7070	.6863	.6654	.6444	.6234
1.00	.8740	.8415	.8087	.7761	.7440	.7128
1.20	1.006	.9586	.9120	.8665	.8229	.7815
1.40	1.123	1.060	.9981	.9398	.8850	.8342
1.60	1.226	1.146	1.070	.9990	.9338	.8748
1.80	1.318	1.220	1.129	1.047	.9727	.9064
2.00	1.397	1.282	1.178	1.086	1.004	.9313
2.50	1.556	1.402	1.269	1.155	1.058	.9739
3.00	1.670	1.483	1.328	1.199	1.091	.9996
4.00	1.813	1.580	1.396	1.248	1.127	1.027
6.00	1.943	1.663	1.452	1.287	1.156	1.049
10.00	2.022	1.711	1.483	1.309	1.171	1.060
∞	2.070	1.740	1.501	1.321	1.180	1.067

$\frac{(M_s)_{\varphi=0}}{M_N}$ for $\varphi=60°$

$M_\infty\delta_N$ \ α/δ_N	0	0.20	0.40	0.60	0.80	1.00
.60	1.021	1.016	1.009	1.001	.9924	.9823
.80	1.021	1.012	1.002	.9906	.9790	.9667
1.00	1.019	1.007	.9941	.9807	.9670	.9530
1.20	1.017	1.003	.9876	.9725	.9572	.9417
1.40	1.016	.9990	.9823	.9658	.9495	.9328
1.60	1.014	.9959	.9781	.9606	.9433	.9258
1.80	1.013	.9935	.9747	.9565	.9384	.9203
2.00	1.012	.9916	.9720	.9531	.9346	.9159
2.50	1.011	.9882	.9672	.9471	.9277	.9086
3.00	1.010	.9862	.9643	.9435	.9235	.9041
4.00	1.009	.9839	.9610	.9394	.9189	.8994
6.00	1.008	.9826	.9584	.9362	.9153	.8958
10.00	1.007	.9811	.9574	.9345	.9135	.8939
∞	1.007	.9805	.9561	.9334	.9123	.8928

$\frac{(M_s)_{\varphi=0}}{M_N}$ for $\varphi=150°$

$M_\infty\delta_N$ \ α/δ_N	0	0.20	0.40	0.60	0.80	1.00
.60	1.021	.9977	.9716	.9436	.9132	.8797
.80	1.021	.9849	.9467	.9060	.8626	.8150
1.00	1.019	.9720	.9228	.8709	.8168	.7559
1.20	1.017	.9606	.9021	.8408	.7758	.7042
1.40	1.016	.9511	.8852	.8161	.7424	.6618
1.60	1.014	.9434	.8716	.7964	.7158	.6277
1.80	1.013	.9373	.8609	.7808	.6942	.5999
2.00	1.012	.9324	.8525	.7686	.6774	.5782
2.50	1.011	.9241	.8379	.7481	.6502	.5429
3.00	1.010	.9190	.8305	.7381	.6368	.5266
4.00	1.009	.9138	.8234	.7313	.6318	----
6.00	1.008	.9101	.8199	---	---	----
10.00	1.007	.9082	.8194	---	---	----
∞	1.007	.9023	---	---	---	----

$\frac{(M_s)_{\varphi=0}}{M_N}$ for $\varphi=0°$

$M_\infty\delta_N$ \ α/δ_N	0	0.20	0.40	0.60	0.80	1.00
.60	1.021	1.024	1.025	1.025	1.026	1.025
.80	1.021	1.022	1.023	1.023	1.022	1.022
1.00	1.019	1.020	1.020	1.020	1.019	1.019
1.20	1.017	1.018	1.018	1.018	1.017	1.017
1.40	1.016	1.016	1.016	1.016	1.016	1.016
1.60	1.014	1.015	1.015	1.015	1.015	1.015
1.80	1.013	1.014	1.014	1.014	1.014	1.014
2.00	1.012	1.013	1.013	1.013	1.013	1.014
2.50	1.011	1.011	1.012	1.012	1.012	1.013
3.00	1.010	1.010	1.011	1.012	1.012	1.012
4.00	1.009	1.009	1.010	1.011	1.011	1.012
6.00	1.008	1.009	1.010	1.010	1.011	1.011
10.00	1.007	1.008	1.009	1.010	1.011	1.011
∞	1.007	1.008	1.009	1.010	1.010	1.011

$\frac{(M_s)_{\varphi=0}}{M_N}$ for $\varphi=90°$

$M_\infty\delta_N$ \ α/δ_N	0	0.20	0.40	0.60	0.80	1.00
.60	1.021	1.009	.9941	.9769	.9573	.9347
.80	1.021	1.001	.9804	.9566	.9302	.9002
1.00	1.019	.9940	.9670	.9377	.9056	.8693
1.20	1.017	.9871	.9555	.9221	.8853	.8437
1.40	1.016	.9812	.9463	.9095	.8693	.8237
1.60	1.014	.9767	.9389	.8995	.8565	.8078
1.80	1.013	.9730	.9330	.8916	.8466	.7959
2.00	1.012	.9700	.9283	.8854	.8389	.7870
2.50	1.011	.9648	.9202	.8745	.8263	.7726
3.00	1.010	.9616	.9152	.8684	.8191	.7652
4.00	1.009	.9581	.9099	.8617	.8119	.7592
6.00	1.008	.9554	.9046	.8567	.8088	.7567
10.00	1.007	.9539	.9038	.8559	.8054	.7563
∞	1.007	.9530	.9023	.8529	.8043	---

$\frac{(M_s)_{\varphi=0}}{M_N}$ for $\varphi=180°$

$M_\infty\delta_N$ \ α/δ_N	0	0.20	0.40	0.60	0.80	1.00
.60	1.021	.9960	.9688	.9405	.9107	.8795
.80	1.021	.9817	.9423	.9008	.8584	.8157
1.00	1.019	.9687	.9168	.8636	.8097	.7547
1.20	1.017	.9566	.8947	.8316	.7680	.7042
1.40	1.016	.9465	.8766	.8052	.7332	.6631
1.60	1.014	.9384	.8620	.7840	.7047	.6309
1.80	1.013	.9319	.8505	.7672	.6821	.6064
2.00	1.012	.9267	.8415	.7540	.6640	.5889
2.50	1.011	.9178	.8264	.7321	.6351	.5693
3.00	1.010	.9126	.8183	.7218	.6212	----
4.00	1.009	.9072	.8114	.7165	.6192	----
6.00	1.008	.9034	.8092	---	---	----
10.00	1.007	.9018	---	---	---	----
∞	1.007	.9007	---	---	---	----